

Deanship of Graduate Studies

Al-Quds University



**Design of Novel Gabapentin Prodrugs by Computational
Methods**

Hanadi Abd Alkareem Sinokrot

M. Sc. Thesis

Jerusalem-Palestine

1440/2019

Design of Novel Gabapentin Prodrugs by Computational Methods

Prepared By

Hanadi Abd Alkareem Sinokrot

B. Sc., Pharmacy, Hebron University, Palestine

Supervisor

Prof. Dr. Rafik Karaman

A Thesis Submitted in Partial Fulfillment of Requirements for
the Degree of Master of Pharmaceutical Science, Al-Quds
University.

1440/2019

Al-Quds University
Deanship of Graduate Studies
Pharmaceutical Science Program



Thesis Approval

Design of Novel Gabapentin Prodrugs by Computational Methods

Prepared by: Hanadi Abd Alkareem Sinokrot

Registration No.: 21511516

Supervisor: Prof. Dr. Rafik Karaman

Master thesis Submitted and Accepted, Date: 25\5\2019

The names and signatures of the examining committee members are as follows:

- 1- Head of Committee: Prof. Rafik Karaman
- 2- Internal Examiner: Dr. Saleh Jbour
- 3- External Examiner: Dr. Hatem Hejaz

Signature:.....

Signature:.....

Signature:.....

Jerusalem–Palestine

1440/2019

Dedication

I would like to thank my family, my mother, father, sisters, and brothers who stood solid to help me through the long years I spent with them. I am very grateful for their support, love, and prayers that were the driving force for my success.

To my colleagues and friends in the Department of Pharmaceutical Sciences. I thank them for their companionship.

Last, but not least, Special thanks to my husband, my daughters Bushra and Eleen for their support; they were always with me and in close proximity to help and without their assistance and support this work would not have been possible.

.

Declaration

I certify that the thesis submitted for the degree of master is a result of my own research, except where otherwise acknowledged, and that this thesis (or any part of the same) has not be submitted for a higher degree to any other university or institution.

Signed:

Hanadi Abd Alkareem Sinokrot

Date: 25/May/2019

Acknowledgment

I would like to thank my Supervisor Professor Rafik Karaman for his guidance, great support and kind advice throughout my master research study.

Hanadi Sinokrot

Abstract

The anti-epileptic Gabapentin has a dose-dependent bioavailability as it is absorbed from the limited distributed and saturable L-amino acid transporter. Drug derivatization using prodrug approach has been demonstrated as a very important means to overcome such related pharmacokinetic and pharmaceutical drawbacks. However, in this approach, enzymes are mandatory for the interconversion of many prodrugs and many prodrug-activating enzymes may be decreased or increased due to genetic polymorphism and age-related physiological changes. Unraveling the mechanisms of a number of enzyme models (intramolecular processes) has contributed to the design of efficient prodrug linkers that can be covalently attached to commonly used drugs; these drugs have the ability to release the active drug chemically, but not enzymatically. Such enzyme models were utilized in my prodrug design approach which was accomplished using computational calculations based on molecular orbital and molecular mechanics methods.

Using DFT molecular orbital at B3LYP 6-31G (d, p) level and molecular mechanics (MM2) calculations of the intramolecular proton transfer in a number of Kirby's enzyme models four Gabapentin prodrugs were designed to provide a medicine with higher bioavailability than its parent drug (Gabapentin), and to provide systems having the potential to release Gabapentin in a controlled matter.

It was found that the intramolecular proton transfer rate of the designed Gabapentin **ProD1-ProD4** is largely determined on the strain energies of the reactions' tetrahedral intermediates; no correlation was found between the cyclization rate and distance between the two reactive centers (r_{GM}). Therefore, the intra-conversion rates of the Gabapentin prodrugs can be programmed according to the nature of the prodrug linker.

Table of contents

Dedication	IV
Declaration	I
Acknowledgment	II
Abstract	III
Table of contents	IV
List of Tables.....	VI
List of Figures	VI
List of Charts.....	VII
List of Abbreviation	VIII
Chapter One (Introduction)	1
1.1 Background.....	2
1.2 Gabapentin.....	6
1.3 Research Problem	7
1.4 Thesis Objectives.....	8
1.4.1 General Objective	8
1.4.2 Specific Objective.....	8
1.5 Research Questions.....	8
Chapter Two (Literature review).....	10
2.1 Prodrugs.....	11
2.2 Enzyme Models Used in the Prodrug Design.....	12
2.3 Computationally Designed Gabapentin Prodrugs Based on Intramolecular Amide Hydrolysis of Kirby's Enzyme Models	15
Chapter Three(Computational Design)	20
3.1 Calculation Programs	21
3.1.1 Arguslab.....	21
3.1.2 Gaussian2009	22
3.2 Calculation Methods.....	23
Chapter Four(Results and Discussion).....	26
4.1 General Consideration	29
4.2 Optimized Geometries for the Entities Involved in the Acid-Catalyzed Hydrolysis in Gabapentin ProD1- ProD4.....	30
4.2.1 Global Minimum Geometries (GM)	30
4.4.2 Transition State Geometries (TS):	31

4.3 The role of the strain energy of the intermediates (E_{sINT}) on the rate of the proton transfer in processes Gabapentin ProD1-ProD4.....	34
Chapter Five(Conclusions and Future Directions).....	38
5.1 Conclusions	39
5.2 Future Directions	39
References	40
Supplementary Material	49
Abstract in Arabic	خطأ! الإشارة المرجعية غير معرفة.

List of Tables

Table 1: DFT (B3LYP) calculated properties of transition states and ground states for the proton transfer reactions in Gabapentin ProD1-ProD4 in gas phase.	32
Table 2: DFT (B3LYP) calculated properties of transition states and ground states for the proton transfer reactions in Gabapentin ProD1-ProD4 in water phase.	33
Table 3: DFT (B3LYP/6-31G (d,p) calculated kinetic and thermodynamic properties for the proton transfer in Gabapentin ProD1-ProD4.	33
Table 4: DFT (B3LYP) calculated kinetic and thermodynamic properties for the acid-catalyzed hydrolysis of 1-7 N-alkylmaleamic acid and Gabapentin ProD1- ProD4.	36

List of Figures

Figure 1: Chemical structure of Gabapentin	6
Figure 2: Chemical structures of Nalkylmalic acids 1-7	16
Figure 3: Proposed Gabapentin Prodrugs Design	17
Figure 4: Linkers used in the Gabapentin Prodrugs	18
Figure 5: Acid - catalyzed hydrolysis of Gabapentin prodrugs (ProD1-ProD4)	19
Figure 6: Proposed mechanism for the hydrolysis of Gabapentin ProD1	28
Figure 7: DFT optimized structures for the global minimum (GM) structures in Gabapentin ProD1-ProD4	30
Figure 8: DFT optimized structures for the transition state (TS) structures in the intramolecular proton transfer reaction of Gabapentin ProD1-ProD4	31
Figure 9: Plot of the DFT calculated ΔG^\ddagger VS. Steric energy for intermediate in water phase for Gabapentin ProD1-ProD4	34
Figure 10: Plot of the DFT calculated ΔG^\ddagger VS. Steric energy for intermediate in gase phase for Gabapentin ProD1-ProD4	35
Figure 11: Plot of the DFT calculated ΔG^\ddagger V.S Relativerate (log K_{rel}) in 1-7 N-alkylmaleamic acid.....	37
Figure 12: Plot of the steric energy for intermediates of 1-7 -N-alkylmaleamic acid vs. relative rate (log K_{rel}).....	37

List of Charts

Chart 1: Schematic representation of the reactants in the cyclization reactions of Gabapentin prodrugs. (r_{GM}) is the distance between the nucleophile (O1) and the electrophile (C6).....	24
--	----

List of Abbreviation

Abbreviations	Definition
GM	Global Minimum
TS	Transition State
INT	Tetrahedral Intermediate
P	Product
ProD	Prodrug
Es	Strain Energy
GP	Gas Phase
H ₂ O	Water Phase
r _{GM}	Distance in the Global Minimum
ΔG^\ddagger	Activation Energy
MM	Molecular Mechanics
QM	Quatum Mechanics
DFT	Density Functional Theory
SN ₂	Nucleophilic Substitution Reaction

Chapter One

Introduction

Chapter One

Introduction

1.1 Background

Generally, a drug is characterized by its biological and physicochemical properties. Drugs, with unsuitable physicochemical properties, might provide inefficient and undesirable therapeutic profiles. Nowadays, finding a drug with good physicochemical properties and pharmacokinetic profile is considered as one of the most important issues in the drug discovery field.

Presently several known oral medicines suffer from poor pharmacokinetic and bioavailability profiles. Therefore, for drugs clinical profiles to be improved, the physicochemical properties of those parent drugs should be modified. The pharmacokinetic or pharmacological barrier's such as low absorption, lack of site specificity, insufficient chemical stability, poor solubility, toxicity, and unacceptable taste/odor should be greatly eliminated [1].

Among the various approaches to minimize the undesirable drug properties while retaining the desirable therapeutic activity is the prodrug approach [2, 3]. Prodrug design is an efficient approach which is based on transiently modified drug's pharmaceutical properties to overcome some of the related pharmacokinetic and pharmaceutical problems [4]. The prodrug approach has been successfully applied to a wide variety of drugs; about 10% of worldwide marketed drugs can be classified as prodrugs [1, 5, 6].

Generally, prodrugs can release their active drugs by two main prodrugs approaches: the traditional approach by which a prodrug interconversion occurs via enzymatic reaction and the novel approach which is based on enzyme models (intramolecular process) that have been advocated to assign the factors playing a dominant role in enzyme catalysis [7-9]. In this approach, there is no need for an enzyme to catalyze the prodrug interconversion. The interconversion rate is determined only by the factors govern rate-limiting step of the intramolecular process [7, 10, 11]. In this novel approach, the design of prodrug is accomplished using computational calculations (computational chemistry) based on

molecular orbital and molecular mechanics methods and correlations between experimental and calculated rate values for some intramolecular processes [7, 10].

Computational chemistry uses the principles of computer science to assist in solving chemical problems. It uses the theoretical chemistry results incorporated into efficient computer programs for calculating the structures, physical and chemical properties of molecules. Few decades ago, the world has viewed an increasing number of medicinal chemists, biochemists and further researchers in various fields who have started using computational methods to better understand the mechanism of intramolecular processes for a number of enzyme models as well as calculating molecular properties of ground and transition states and design of some novel prodrug linkers. The application of computational chemistry has many advantages mainly by helping to reduce the need for access to expensive laboratory time, test equipment and chemicals [10, 12, 13].

Today, modern computational methods such as those based on quantum mechanics (QM) and molecular mechanics (MM) methods could be exploited for the design of innovative prodrugs for common use drugs [10].

Quantum Mechanics (QM):

Quantum Mechanics (QM also known as Quantum Physics, or Quantum Theory) is the laws of physics for very small and light objects, such as electrons and nuclei. It can provide a mathematical description of the behavior of electrons and thus of chemistry. In QM, the Schrodinger equation is solved for the wave-functions of our particles, giving information about the probability of measuring various values for its physical properties [14, 15].

$$\hat{H} \Psi = E \Psi \rightarrow \text{Schrodinger Equation}$$

The Hamiltonian operator, H, depends on the kinetic and potential energies of the nuclei and electrons in the atom or molecule. The wave-function, Ψ , will give us information about the probability of finding the electrons in different places in the molecule. The energy, E, is related to the energies of individual electrons which can be used to help interpret electronic spectroscopy.

The Quantum mechanics includes *ab initio*, semi-empirical and Density Functional Theory (DFT) methods [16-18].

Ab initio Methods

Ab initio is an essential calculation method based on a computational solution of the electronic Schrodinger equation by a well-defined approximation (a “model chemistry”) [4]. When all approximations are sufficiently small in magnitude, and when the finite set of basic functions tends toward the limit of a complete set, we can use the *ab initio* method. *Ab initio* electronic structure methods have the advantage of making converge to the exact solution. This method is used to determine the positions of a collection of atomic nuclei, the total number of electrons in the system, calculate the electronic energy, electron density, and more properties of systems containing tens, or even hundreds of atoms. However, the treatment of large condensed-phase systems (e.g., proteins in aqueous solution) entirely by *ab initio* methods is extremely expensive computationally; they take a significant amount of computer time, memory, and disk space.

Semi-Empirical Methods

The semi-empirical quantum methods depend on the Hartree–Fock formalism, and they are very important in the study of systems (large molecules) that are out of reach of more accurate methods [19]. Semi-empirical calculations are much faster than their *ab initio* counterparts. The most used semi-empirical methods are MINDO, MNDO, MINDO/3, AM1, PM3, and SAM1[20].

Semi-empirical methods make many approximations; their results can be trust-worthy and accurate only when the molecule being computed is close enough to the molecules in the database used to parameterize the method.

Density Functional Theory

The Density Functional Theory (DFT) is another widely used, popular and useful quantum mechanical modeling method available in physics and chemistry. In this theory, the energy of the molecule is a functional of the electron density, where the electron density is a function with three variables— x -, y -, and z -position of the electrons, and the determination of the electron density is independent of the number of electrons [16, 21].

DFT can be used to determine the properties of many-electron systems with a significant increase in computational accuracy but without the additional increase in computing time. It is used to calculate electronic structures (principally the ground state) and energies for medium-sized systems (30–60 atoms) of biological and pharmaceutical interest but is not restricted to the second row of the periodic table [21].

Nevertheless, problems such as the incomplete treatment of dispersion can adversely affect the DFT degree of accuracy in the treatment of systems which are dominated by dispersion. Moreover, the need to determine the most appropriate method for a particular application force the practitioner to consult the literature, prior to choosing a DFT method, to determine the suitability of that choice for that particular problem or application.

DFT methods such as B3LYP/6-31G(d) are oftentimes considered to be standard model chemistry for many applications. However, Some DFT methods are specifically designed for specific applications, such as the MPW1K hybrid method which is designed for the determination of kinetics problems.

Molecular mechanics

Molecular mechanics is a mathematical approach used to calculate the energy, optimized geometry, dipole moment, and many other physical properties of a given molecule. Macromolecules such as proteins, large crystal structures, and relatively large solvated systems are widely calculated by this method. Molecular mechanics is fast, and large molecule like a steroid (e.g. cholesterol) can be optimized only in a few seconds on a powerful desktop computer. However, determination of parameters, such as a large number of unique torsion angles present in structurally diverse molecules, makes a limitation for this method [12].

In order to investigate the functional mechanisms of biological macromolecules based on their 3D and electronic structures, *ab initio* methods are preferable to be utilized. However, the treatment of large systems (e.g., proteins in aqueous solution) entirely by *ab initio* methods is extremely expensive computationally. The size of the system, which *ab initio* calculations can handle, is relatively small despite the large sizes of bio-macromolecules surrounding solvent water molecules. Accordingly, *ab initio* calculations can be used in isolated models of areas of proteins such as active sites. Whereas the remainder can be treated more approximately by means of Molecular Mechanics (MM). The technologies for coupling quantum chemical methods to molecular mechanic methods [mixed quantum mechanics (QM)/MM] have become an essential component of the theoretical arsenal, enabling realistic modeling of even the most complex molecular structures [22].

1.2 Gabapentin

Gabapentin is 1-(aminomethyl)cyclohexaneacetic acid (Figure 1) with a molecular weight of 171.237 g/mol and a molecular formula of $C_9H_{17}NO_2$. It has a dose-dependent bioavailability (27-60%).

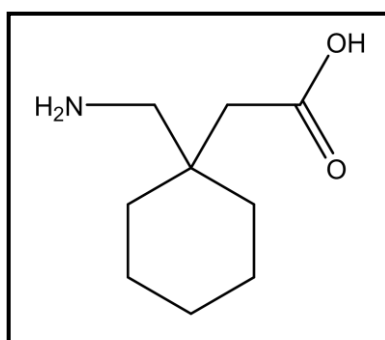


Figure 1: Chemical structure of Gabapentin

Gabapentin, a structural analog of GABA (gamma-aminobutyric acid), is an anti-epileptic used for the treatment of epilepsy [23] and neuropathic pain [24, 25]. Although its exact mode of action is not entirely known, gabapentin appears to have a unique effect on voltage-dependent calcium ion channels at the postsynaptic dorsal horns. It may inhibit the alpha-2-delta ($\alpha_2\delta$) subunit of the N-type voltage-dependent calcium ion channels on neurons. After the binding to the $\alpha_2\delta$ subunit, it reduces calcium influx that is needed for the release of neurotransmitters-especially excitatory amino acid- from presynaptic

neurons. This channel becomes up-regulated when nerves are stimulated, such as in epileptic conditions or associated with neuropathology [26].

Despite that the gabapentin has a similarity in structure to GABA; there is no direct interaction between gabapentin with GABA receptors. [27] Gabapentin is not bind to GABAA or GABAB receptors and is not an inhibitor of GABA uptake or degradation [28].

Gabapentin is an amino acid that exists at physiological pH as a zwitterion as it is doubly charged; its native permeability to membrane barriers within the body is low as its water soluble and GI tract absorption are binding to the L gamma amino acid transport system in the proximal small bowel. However, gabapentin molecules can cross membrane barriers more easily because it is a substrate of the system L transporter of the gut and a small amount of gabapentin transported via passive diffusion [29-31].

1.3 Research Problem

The bioavailability of gabapentin is dose-dependent as the drug is absorbed from the proximal small bowel into the blood stream by the L-amino acid transport system and because this transport system is capacity limited [29].

Dose-dependent pharmacokinetics, high variability between patients, and potentially ineffective drug exposure occurs due to the fact that the absorption of gabapentin occur in a limited region of the small intestine and at clinically used doses it saturates [22, 32].

Surprisingly, the bioavailability of gabapentin decreases with increasing dosages; the oral bioavailability of gabapentin is approximately 60%, 34%, 33%, and 27% following 900, 1200, 3600, and 4800 mg/day given in 3 divided doses, respectively. Most importantly, the range of doses where bioavailability decreases concur with doses reported being useful for the treatment of neuropathic pain [33].

However, the effectiveness of Gabapentin is limited as a result of inherent pharmacokinetic deficiencies. The variability of Plasma exposure to gabapentin after oral dosing due to saturation of its absorption pathway, a low-capacity transporter found only in the upper small intestine make it unpredictable and lack of absorption in the large intestine is another problem with gabapentin saturates [32].

Saturation of the gabapentin transport pathway may be responsible for the observed dose-dependent, and this causes a decrease in bioavailability. Gabapentin absorption is mediated by a low-capacity solute transporter, probably an L-type amino acid transporter which is located mainly in the upper small intestine [33].

As a result, the prediction of the Gabapentin dose necessary to achieve an optimal therapeutic effect in a given patient is often difficult, and the desired treatment response may not be achieved. One of the causes that necessitate the frequent dosing is the short half-life of gabapentin (about 5–7 h) which is a cause of noncompliance in epileptic patients and missed doses which can reduce clinical effectiveness [32, 33].

1.4 Thesis Objectives

1.4.1 General Objective

The main goal of this research was to design prodrugs, with a better bioavailability and having the potential to release their parent drug in a controlled manner using a variety of different molecular orbital and molecular mechanics methods and correlations between experimental and calculated reactions rates.

1.4.2 Specific Objective

► Calculations of Kirby's enzyme model mechanism for the design of Gabapentin prodrugs which should have the following properties:

- 1- Converted to Gabapentin in a controlled manner.
- 2- The linker attached to the drug moiety and the whole Gabapentin prodrug moiety should have no toxicity and safe.
- 3- To provide systems with enhanced bioavailability compared to the parent Gabapentin.

1.5 Research Questions

1. Would the DFT calculation method for Gabapentin prodrugs be capable of producing reaction rates similar to that obtained by Kirby?

2. Would the DFT calculations be good methods for the design of Gabapentin prodrugs that can be cleaved in physiological environments to furnish the active drugs and a non-toxic moiety and have better bioavailability than their parent drug?

Chapter Two

Literature Review

Chapter Two

Literature Review

2.1 Prodrugs

A drug is a chemical entity which is used in the treatment, prevention and/or diagnosis of disease. Generally, a drug is characterized by its biological and physicochemical properties such as solubility and polarity, thus a drug with good properties results in efficient bioavailability and consequently effective treatment of disease. However, several studies have shown that many known oral medicines suffer from disagreeable pharmacokinetic and bioavailability profiles which are attributed to the undesirable physicochemical properties. Therefore, these issues should be significantly considered early in the drug discovery process to improve the drug's therapeutic efficacy and cost-effectiveness.

An important approach that has been developed to modify and improve various undesirable physicochemical properties is a prodrug design. The prodrug approach, that was first introduced by Albert, can be used to synthesize new chemical entities that have superior efficacy, selectivity, and reduced toxicity. Hence an optimized therapeutic outcome can be accomplished.

Actually, around 10% of all marketed drugs are prodrugs, 20% of small molecular weight drugs approved between 2000 and 2008 were prodrugs, and about 12% was the share of prodrugs in the drug market between 2008 and 2017 [34].

The use of the term "prodrug" usually involves a covalent link between a drug and a chemical moiety (linker) that can be enzymatically or chemically degraded *in vivo* to release the parent active drug which can exert the desired therapeutic effect. Ideally, the prodrug should be converted to the parent drug and non-toxic moiety as soon as its goal is achieved followed by the subsequent rapid elimination of the released linker group [2, 35].

In some prodrug strategies, the target is to improve the pharmacokinetic profile like absorption of the original drug by altering in their physicochemical parameters, like lipophilicity (HLP Balance) through the linking of specific functional groups or macromolecules to the naked drugs [36-41]. Other prodrug strategies aim to make targeting drugs [42] or make drugs more resistant to hydrolysis and metabolism by the

addition of a bulky alkyl group like t-butyl in close proximity to the functional group [43, 44], or by removing or replacing a metabolically vulnerable group [45].

The major challenge facing the prodrug approach strategy is that enzymes are mandatory for the interconversion of many prodrugs to their active parent drugs. And many prodrug-activating enzymes may be decreased or increased due to genetic polymorphism, age-related physiological changes, or drug interactions, leading to adverse pharmacokinetic, pharmacodynamics, and clinical effects. In addition, there are wide interspecies variations in both the expression and function of the major enzyme systems activating prodrugs.

However, to overcome all problems associated with prodrug interconversion by enzymes, a novel chemical approach for drugs that contain hydroxyl, phenol, or amine groups can be used to design prodrugs based on intramolecular processes (enzyme models) that were advocated to assign the factors playing a dominant role in enzyme catalysis [7-9]. In this approach, there is no need for an enzyme to catalyze the prodrug interconversion; the interconversion rate is determined only by the factors governing the rate-limiting step of the intramolecular process [7, 10, 11]. In the novel prodrug approach, the design of prodrug is accomplished using computational calculations (computational chemistry) based on molecular orbital, molecular mechanics methods, and correlations between experimental and calculated rate values for some intramolecular processes [7, 10].

2.2 Enzyme Models Used in the Prodrug Design

The rate of the reactions carried out in the presence of enzyme exceeded non-enzymatic bimolecular counter parts. For example, the rate constant of reactions catalyzed by cyclophilin are enhanced by 10^5 , and those by orotidine monophosphate decarboxylase are enhanced by 10^{17} [46].

This amazing efficiency of the enzyme to catalyze biochemical reactions has motivated many organic chemists and biochemists to study the mechanisms of how enzymes catalyze biochemical reactions via examining particular intramolecular (enzyme model) process [47-52].

During the past sixty years, scientists have provided many studies that interpret how enzymes catalyze biochemical transformations. Today, the consensus is that the catalytic

activity of an enzyme is based on the combined effects of catalysis by functional groups and the ability to reroute intermolecular reactions through alternative pathways by which substrates bind to preorganized active sites.

The significant rate of acceleration achieved by enzymes is related to the binding of the substrate within the confines of the enzyme pocket called the active site. The binding energy of the resulting enzyme-substrate complex is the main driving force and the most important contributor to catalysis. This binding energy is used to overcome prominent physical and thermodynamic factors that create barriers for the reaction (ΔG) in all bio-conversions catalyzed by enzymes.

In the past five decades, proposals have been made from attempts to interpret changes in reactivity versus structural variations in intramolecular systems. Among these proposals and hypothesis are the following:

- (I) “Orbital steering” proposed by Koshland, it suggests a rapid intramolecularity arises from a severe angular dependence of organic reactions, such as in the lactonization of rigid hydroxy acids [53].
- (II) “Proximity orientation” in intramolecular processes (near attack conformation) as proposed by Bruice and demonstrated in the lactonization of di-carboxylic acids semi-esters [54-56].
- (III) “Stereopopulation control” based on the concept of freezing a molecule into a productive rotamer as advocated by Cohen [57-59].
- (IV) Manger’s “spatiotemporal hypothesis” which postulates that the rate of reaction between two reactive centers is proportional to the time that the two centers reside within a critical distance [60-64].
- (V) Kirby’s proton transfer models on the acid-catalyzed hydrolysis of acetals and N-alkylmaleamic acids which demonstrated the importance of hydrogen bonding formation in the products and transition states leading to them [8, 65-72].

Understanding these intramolecular processes can draw a basis for utilizing these enzyme models as linkers to certain drugs for synthesizing of prodrugs that they will undergo non-enzymatic (chemical) conversion to their parental drugs in predicted rates and with higher bioavailability than their corresponding parental drugs.

Many prodrugs were designed using Kirby's enzyme model, such as the anti-malarial Atovaquone [73], antihypertensive atenolol [74], tranexamic acid for treatment of heavy bleeding conditions [75], antibacterial cefuroxime [76] and the antiviral acyclovir prodrugs [77]. In addition to the use of Menger's Kemp acid enzyme model to design of dopamine prodrugs for the treatment of Parkinson's disease [78]. As well, prodrugs for masking the unpleasant taste of atenolol (anti-hypertensive) [74] and the bitterless paracetamol were designed, synthesized and their kinetics were studied [74].

The calculations study on Kirby's acetals enzyme model also directed to the design of novel prodrug such as, aza-nucleoside (to treat myelodysplastic syndromes) [92], the decongestant phenylephrine [13], atovaquone [73, 79, 80] and statins for treatment of high cholesterol levels in the blood [81]. In these prodrugs, the hydroxyl group of the active drug was linked to the acetal moiety upon the exposure of such prodrug to the physiological environment; it has the potential to convert to its parent active form with rates that are solely determined on the structural features of the linker (Kirby's acetal).

Recently, Karaman's group has explored the mechanistic pathways of a number of intramolecular processes using *ab initio* and density functional theory (DFT) molecular orbital methods [82]. The results obtained were found to be in accordance with that report by Kirby and Lancaster and Kluger and Chin.

Among the studied intramolecular processes are the following:

- ❖ Acid-catalyzed lactonization of hydroxy-acids as researched by Cohen [83] and Menger [84].
- ❖ S_N2 -based ring closing reactions as studied by Brown, Bruice, and Mandolin [85].
- ❖ Proton transfer between two oxygens in Kirby's acetals [76, 86], proton transfer between nitrogen and oxygen in Kirby's enzyme models [76, 86] and proton transfer from oxygen to carbon in some of Kirby's enol ethers [87].

Results of these studies indicate the necessity to further explore the reaction mechanisms in order to determine the factors affecting the reaction rate such as: (1) The driving force for enhancements in the rate of intramolecular processes is both entropy and enthalpy effects. In the cases by which enthalpic effects were predominant such as ring-cyclization and proton transfer reactions proximity or/and steric effects were the driving force for rate

accelerations. (2) The distance between the two reactive centers determine the nature of the reaction being intermolecular or intramolecular (when the distance between the two reacting centers is about 2.4Å, the reaction is intramolecular, whereas when the distance is 3Å and more, the reaction prefers the intermolecular process). (3) In SN₂-based ring-closing reactions leading to three-, four- and five-membered rings the gem-dialkyl effect is more dominant in processes involving the formation of an unstrained five-membered ring, and the need for directional flexibility decreases as the size of the ring being formed increases. (4) Accelerations in the rate for intramolecular reactions are a result of both entropy and enthalpy effects. Finally (5) in Kirby's acetal systems, an efficient proton transfer between two oxygens atoms and between nitrogen and oxygen were affordable when strong hydrogen bonds are developed in the products and the corresponding transition states leading to them [82, 84, 85].

2.3 Computationally Designed Gabapentin Prodrugs Based on Intramolecular Amide Hydrolysis of Kirby's Enzyme Models

Proton transfer reaction is one of the most common processes catalyzed by enzymes. Due to the fact that reactions of an enzyme active site and substrate are related to functional groups held in close proximity, many scientists have encouraged exploiting intramolecularity in modeling enzyme catalysis. Both enzymes and intramolecularity are similar in that the reacting centers are held together, noncovalently with the enzymes, and covalently with the intramolecular process. The tremendous high efficiency of enzymes catalysis depends on a combination of some factors that most of them have been recognized, but none of them was fully understood. Although the devoted research to the chemistry of enzyme catalysis is growing rapidly, a number of several factors remain to be studied [88, 89].

The mechanism of acid-catalyzed hydrolysis of N-alkylmaleamic acid to maleamic acid derivatives and amines (Figure 2) was studied by Kirby. The results have revealed that the amide bond cleavage is due to intramolecular nucleophilic catalysis by the adjacent carboxylic acid group and the rate of hydrolysis was largely dependent on the substitution on the carbon-carbon double bond [90]. The rate-limiting step for the hydrolysis is the dissociation of the tetrahedral intermediate.

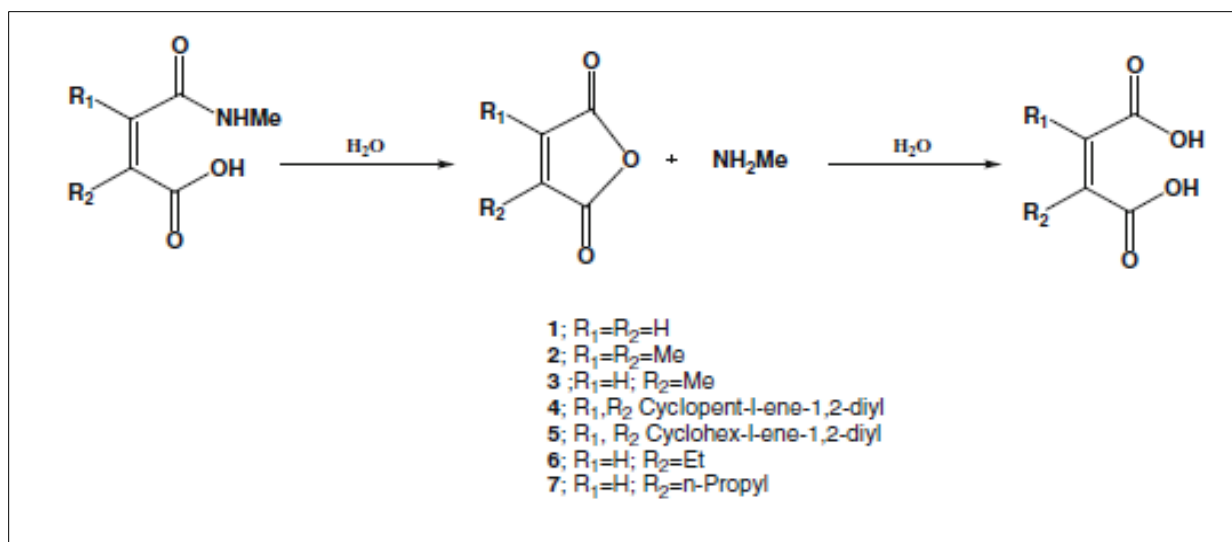


Figure 2: Chemical structures of Nalkylmaleamic acids **1-7**

Based on AM1 semiempirical calculations, in 1990, Katagi had demonstrated that the rate-limiting step is the formation of the tetrahedral intermediate, not its dissociation [91]. Later on, Kluger and Chin investigated that the intramolecular hydrolysis rate-limiting step is a function of both the basicity of the leaving group and the solution acidity [92].

In order to determine the factors playing a dominant role in proton transfer processes, Karaman and coworkers have computationally studied Kirby's intramolecular acid-catalyzed hydrolysis of N-alkylmaleamic acids **1-7** using DFT calculation method. The result confirmed that the reaction proceeds in three steps: the first step is proton transfer from the carboxylic acid to the adjacent amide carbonyl carbon and the second step of the reaction involves nucleophilic attack of the carboxylate anion onto the protonated carbonyl carbon and finally dissociation of the tetrahedral intermediate to provide the product. Moreover, the result demonstrates that the rate-limiting step is dependent on the reaction medium. When the calculations were run in the gas phase, the rate-limiting step was the tetrahedral intermediate formation, whereas when the calculations were conducted in the presence of a cluster of water the rate-limiting step is the dissociation of the tetrahedral intermediate.

Furthermore, the results showed that the efficiency of the intramolecular acid-catalyzed hydrolysis is largely dependent on the substitution of the carbon-carbon double bond, when the leaving group (methylamine) in **1-7** was replaced with a group having a low pK_a

value. The formation of the tetrahedral intermediate is the rate-limiting step, and the rate of hydrolysis was found to be linearly correlated with the strain energy of the tetrahedral intermediate or the product. Systems having strained tetrahedral intermediates or products experience low rates and vice versa [65, 77, 93].

Gabapentin is an amino acid and it is highly charged at physiological pH; both the amino group and the carboxyl group are ionizable, existing as a zwitterion with a pKa 1 of 3.7 and a pKa 2 of 10.7 [31].

Since Gabapentin is doubly-charged and its pKa is outside the range (6-9), Gabapentin tends to be ionized and poorly absorbed through membrane tissue. However, converting the structure of Gabapentin (neutralizing the ionized amine group) into amide prodrugs (Figure 3) will provide a change in the pKa and subsequently an improvement in the absorption [31].

Based on DFT calculations for the acid-catalyzed hydrolysis of several N-alkylmaleamic acid derivatives (Figure 2) four Gabapentin prodrugs were designed (Figure 3) using four linkers (Figure 4).

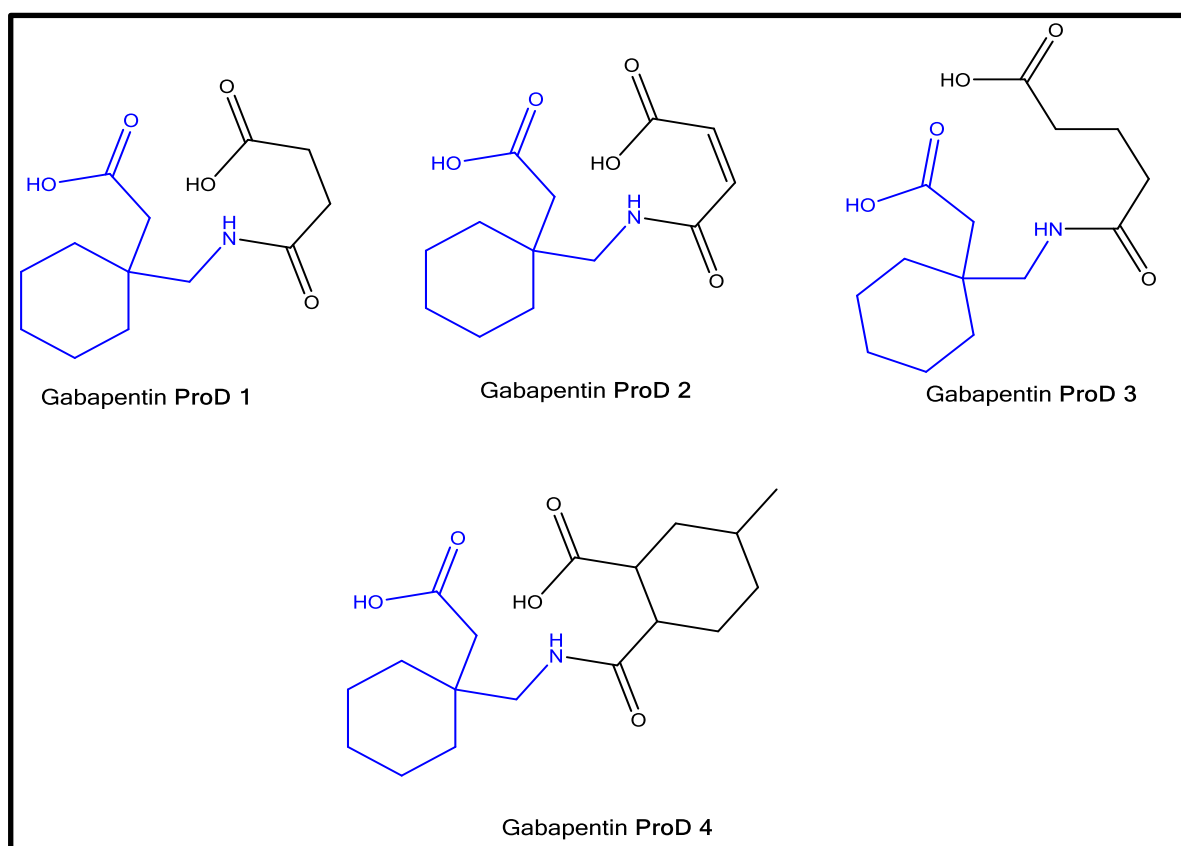


Figure 3: Proposed Gabapentin Prodrugs Design

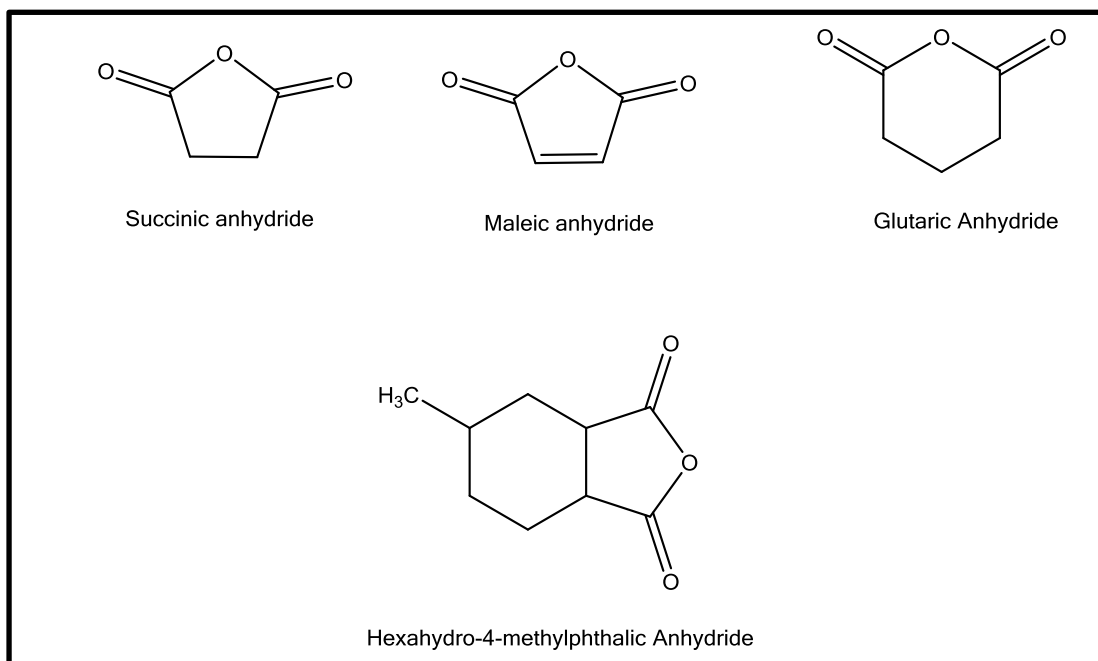


Figure 4: Linkers used in the Gabapentin Prodrugs

As shown in Figure 5, Gabapentin **ProD1-ProD4** have a carboxylic group (hydrophilic moiety) and a lipophilic moiety (the rest of the prodrug) where the combination of both moieties assure a relatively moderate HLB, and which will equilibrate between the ionic and the free acid forms especially in a physiological environment of pH 5.5-6.8 (intestine). Thus, it is expected that Gabapentin **ProD1-ProD4** may have better bioavailability than the parent drug due to neutralizing the ionized amine group which results in absorption improvement. In addition, these prodrugs may be used in different dosage forms (i.e. enteric coated tablets, topical use and etc.) because of their potential solubility in organic and aqueous media due to the ability of the carboxylic group to be converted to the corresponding carboxylate anion in a physiological pH of around 6.0.

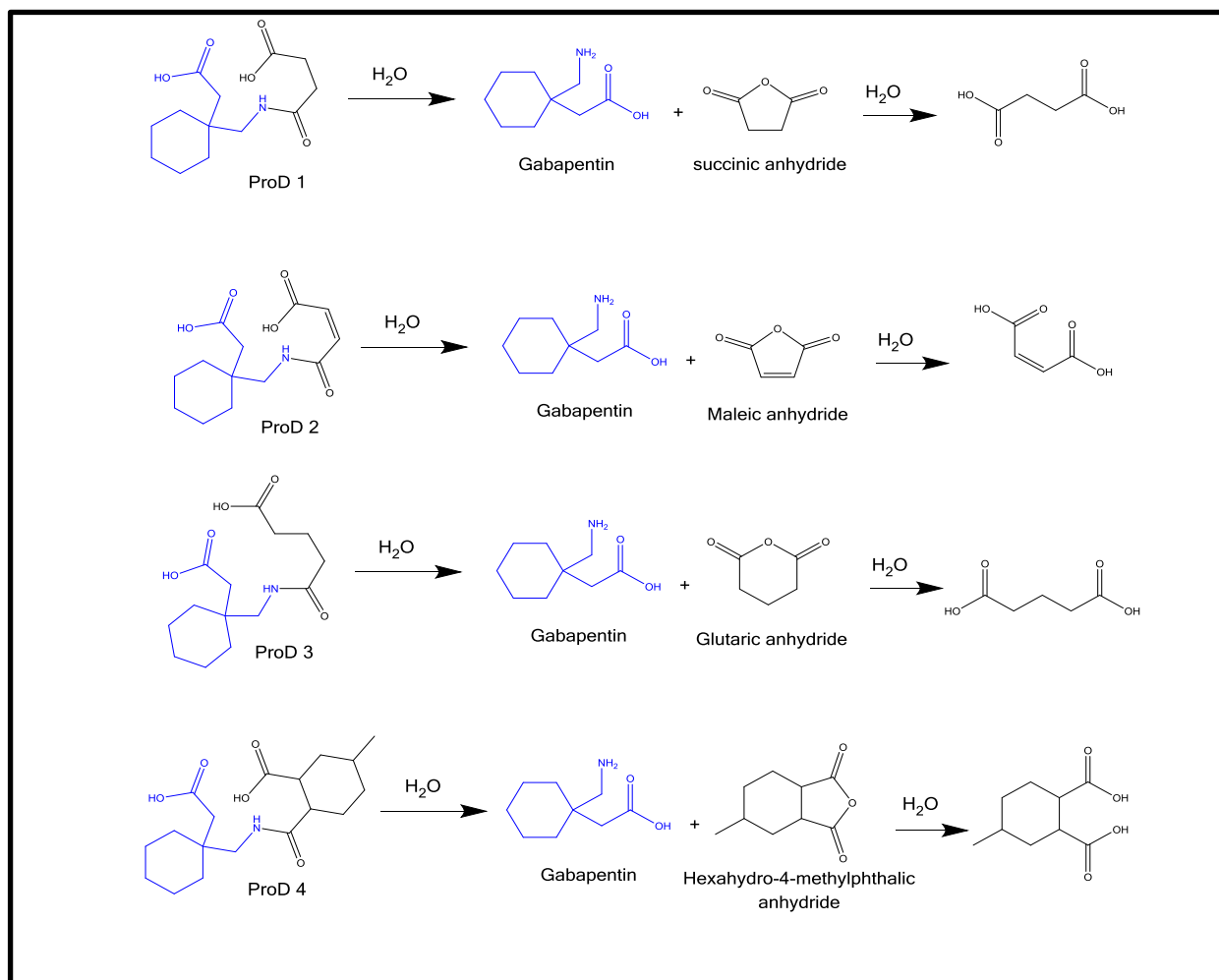


Figure 5: Acid - catalyzed hydrolysis of Gabapentin prodrugs (**ProD1-ProD4**)

Chapter Three

Computational (Design) section

Chapter three

Computational (Design) Section

Calculation Programs and Methods Used in the Thesis

3.1 Calculation Programs

The following programs were exploited in the design calculations:

3.1.1 Arguslab

Arguslab is free molecular modeling, graphics, and drug design program that offers quite good on-screen molecule-building facilities with a moderate library of useful molecules. This program can create 3D geometry optimized models using the UFF force field, as it covers all elements of the Periodic Table because it is not restricted to known atom types in its parameterization, though it does use some common ones. The resulting energies are distinctly different from those obtained using some of the more conventional force fields, and wherever possible one needs to re-optimize at a higher level. For this, Arguslab offers geometry optimization using the MNDO, AM1 or PM3 semi-empirical methods, as well as single point calculations. There are also single point semi-empirical calculations using Extended Huckel (for a bigger element coverage) or ZINDO (for excited states for UV/visible absorption prediction). Version 3.1 of Arguslab has good facilities for calculating electron density or orbital surfaces at the semi-empirical levels and displaying them [94].

Argus lab writes its own format of molecule file, like .xml, but it can also write xyz files for input to other programs, e.g. Molden. It creates (and leaves behind) a lot of temporary files which need to be managed.

To start work using Arguslab, we press the 'New' button (top left) to get a new molecule screen, or press the 'Open' button to read in a molecule which has saved previously in your Argus directory.

In Arguslab, we need to save our molecule with whatever name we want before doing a geometry optimization as well as after ward so that all the ancillary files will have the right

names. If we forget to change the file name before modifying a molecule, files will be saved automatically with the same name used previously. As a problem to this program, it should be noted that not all the required data can be fully saved.

It is best not to maximize the molecule window because then its title bar will display the name by which we are currently saving the files. Just drag its bottom right corner so that it fills most of the Arguslab worktop. To stop using Argus lab, click File Exit, if we have molecule windows open, this will just close one of these. We need to do it repeatedly to close all the windows (if we have several open) and then stop the program.

3.1.2 Gaussian 2009

Gaussian 09 is the latest version in the Gaussian series of electronic structure programs, used by chemists, chemical engineers, biochemists, physicists, and other scientists. It utilizes fundamental laws of quantum mechanics to predict energies, molecular structures, vibration frequencies, and numerous molecular properties for systems in the gas phase and in solution, and it can model their ground state and excited states. The use of Gaussian makes the theoretical study of basic research in established and emerging areas of chemical interest possible, and also to study molecules and reactions of definite or potential interest including both stable species and compounds which are difficult or impossible to observe experimentally either due to their nature (e.g., toxicity, combustibility, radioactivity) or their inherent fleeting nature (e.g., short-lived intermediates and transition structures).

Gaussian 09 takes as an input of the (.gjf) file produced by GaussView and runs the analyzer to produce a solution to the problem. A typical command line for the solver is given below. G09.exe input_file.gjf output_file.out

Checkpoint file: output_file.chk

An output text file (.out) is created so that it can be read and inspected by a human. In addition, a checkpoint file (.chk) is also produced that it may be processed by a computer to produce further detailed information.

Dissecting the output file, the Z-matrix represents how the software knows the molecular geometry (structure). Notice that the molecule has no charge and a multiplicity of 1 (all pairedelectrons). The structure is also represented as a more standard xyz coordinate

system. The distance matrix shows the distance of each atom from the other atoms in units of angstroms.

3.1.3 Molden

Molden is a computational program package made for displaying molecular densities from the *ab initio* packages, Games-US, Games-UK, Gaussian, MOLPRO and from semi-empirical packages such as MOPAC, and supports a number of other formats. Molden can interpret and convert information from all these programs into its own format, thereby providing a standardizing tool. It can display molecular orbitals or electron density as contour plots or 3D grid plots and output to a number of graphical formats, e.g. postscript, X-Windows, VRML, povray, OpenGL, tekronix4014 and hpgl, hp2392. It can animate reaction paths and molecular vibrations. The Molden program can also be used as a visual Z-matrix molecule editor, thereby allowing users to create the molecule of their choice and being able to save the geometry in the Molden format [63]. Molden format incorporates numerous data stores in a text file; each piece of data is headed by a key term e.g. [MO] for molecular orbitals, [STO] for slater type orbital basis sets, plus many others like [GTO], [GEOMETRIES], etc.

Molden format also features a stand-alone force field program (Ambfor) which can optimize geometries with the combined Amber (protein) and GAFF (small molecules) force fields. Atoms type can be done automatically and interactively from within Molden as well as firing optimization jobs.

3.2 Calculation Methods

The Becke three-parameter, hybrid functional combined with the Lee, Yang, and Parr correlation functional, denoted B3LYP, were employed in the calculations using density functional theory (DFT). All calculations were carried out using the quantum chemical package, Gaussian-2009, and based on the restricted Hartree-Fock method [95]. The starting geometries of all calculated molecules were obtained using the Argus Lab program [96] and were initially optimized at the HF/6-31G level of theory followed by optimization at the B3LYP/6-31G(d,p). Total geometry optimizations included all internal rotations.

Second derivatives were estimated for all 3N-6 geometrical parameters during optimization. The search for the global minimum structure, in each of the systems studied, was accomplished by 36 rotations of the carboxyl group about the bond C₃-C₄ in increments of 10° (i.e. the variation of the dihedral angle C₂C₃C₄C₅, see Chart 1) and calculation of the energies of the resulting conformers.

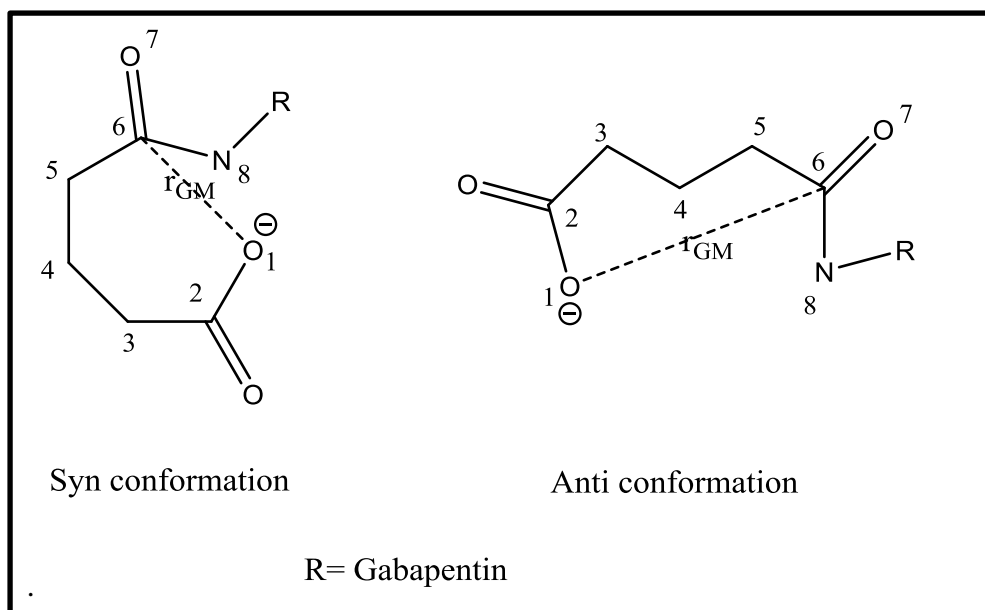


Chart 1: Schematic representation of the reactants in the cyclization reactions of Gabapentin prodrugs. (r_{GM}) is the distance between the nucleophile (O1) and the electrophile (C6).

An energy minimum (a stable compound or a reactive intermediate) has no negative vibrational force constant. The Reaction Coordinate Method [97] was used to calculate the activation energy in Gabapentin **ProD1-ProD4**. The transition state structures for all systems studied were obtained from the increase in the distance between the phenolic oxygen (O) and the carbonyl carbon (C) in increments of 0.1 Å (see Chart1). The activation energy values for the cyclization reactions of all di-carboxylic semi-esters were calculated from the difference in energies of the global minimum structures (GM) and the derived transition states (TS). The transition state structures were verified by their only one

negative frequency. Full optimization of the transition states was accomplished after removing any of the constraints imposed while executing the energy profile. The activation energies, obtained from the DFT at B3LYP/6-311 + G (d,p) level of theory for all molecules, were calculated with and without the inclusion of solvent (dielectric constant of 78.39, water). The calculations, with solvent, were performed using the integral equation formalism model of the Polarizable Continuum Model (PCM) [98-102]. In this model, the cavity is created *via* a series of overlapping spheres. The employed Radii type was the United Atom Topological Model on Radii optimized for the PBE0/6-31G (d) level of theory.

Chapter Four

Results and Discussion

Chapter Four

Result and Discussion

The kinetic study for the acid-catalyzed hydrolysis of N-alkylmaleamic acids **1-7** by Kirby's group (Figure 2) revealed that the amide bond cleavage occurs due to intramolecular nucleophilic attack which is catalyzed by the adjacent carboxylic acid group; the rate-limiting step is the tetrahedral intermediate dissociation [103].

Karaman's DFT calculations on the acid-catalyzed hydrolysis of Kirby's *N*-alkylmaleamic acids revealed that the rate-limiting step is the collapse of the tetrahedral intermediate in an aqueous medium, whereas the rate-limiting step is the formation of the tetrahedral intermediate in the gas phase. Furthermore, the calculations showed the following:

A correlation between the acid-catalyzed hydrolysis efficiency

1. The difference between the strain energies of intermediate and product, and intermediate and reactant.
2. The distance between the hydroxyl oxygen of the carboxylic group and the amide carbonyl carbon.
3. The angle of attack.

The calculations, moreover, revealed that the acid catalyzed reaction occurred following three steps: (1) proton transfer from the carboxylic group to the adjacent amide carbonyl oxygen, (2) nucleophilic attack of the carboxylate anion onto the protonated carbonyl carbon; and (3) dissociation of the tetrahedral intermediate to provide products (Figure 6).

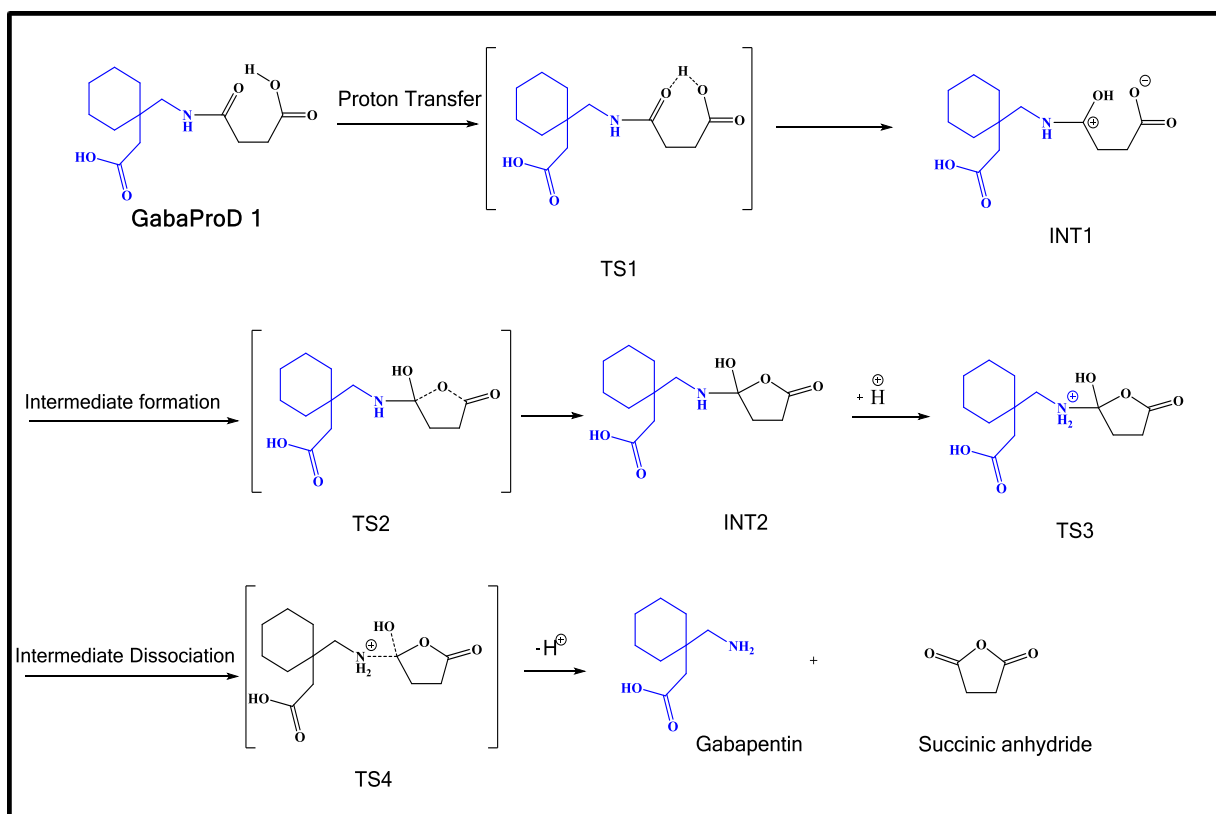


Figure 6: Proposed mechanism for the hydrolysis of Gabapentin **ProD1**

According to the calculation results of Kirby's *N*-alkylmaleamic acids model, I proposed some prodrugs of Gabapentin by linking this drug with anhydride linker such as maleic, succinic, glutaric, and hexahydro-4-methylphthalic (Figure 4) aiming to: (1) improve the bioavailability of the parent drugs, (2) to make prodrug that is capable of releasing the parent drug in a sustained release manner.

As shown in Figure 4, Gabapentin **ProD1-ProD4** have a carboxylic group (hydrophilic moiety) and a lipophilic moiety (the rest of the prodrug) where the combination of both moieties secures a modified HLB.

In this chapter, I reported the DFT at B3LYP 6-31G (d,p) level calculations of ground state and transition state structures, vibrational frequencies, and reaction trajectories for intramolecular proton transfer in Gabapentin prodrugs **ProD1-ProD4**.

Computations were directed toward elucidation of the transition and ground state structures (global minimum, intermediates, and products) for the acid-catalyzed hydrolysis of Gabapentin **ProD1-ProD4** in the gas phase and in the water phase (a dielectric constant of

79.38). It is expected that the stability of the chemical entities (GM, TS, and P.) will be different in the gas phase compared to that in water (a relatively high dielectric constant).

4.1 General Consideration

Continuing the strategy for exploring enzyme models in the design of novel prodrugs, Kirby's enzyme models (Acid-catalyzed hydrolysis) was employed in the design of Gabapentin prodrugs (Figure 5) with the potential to be more bioavailable than their active parent drug. Furthermore, it is planned that the intraconversion rate of Gabapentin prodrugs to Gabapentin can be programmed according to the nature of the prodrug linker.

Because the free energy of the reactant is strongly dependent on its conformation. The orientation of the carboxylate anion to the amide carbonyl moiety is very important and affecting the mode and rate of the cyclization reaction. Therefore, the identification of the most stable conformer (Global Minimum, GM) for each of Kirby's N-alkylmaleamic acids **1–7** and Gabapentin prodrugs **ProD1–ProD4** are crucially important. The global minimum search was achieved by 360 rotation of the carboxylic group about the C₃-C₄ bond (i.e. the variation of the dihedral angle C₂C₃C₄C₅ see Chart 1) and calculation of the conformational energies.

In the DFT calculations of the starting geometries in Gabapentin **ProD1–ProD4**, two different types of conformations were considered: one in which the carboxylic hydroxyl proton is *syn* to the amide group and another in which it is *anti* (Chart 1). The global minimum search for Gabapentin **ProD1–ProD4** revealed that all of them exist in the *syn* orientation (Figure 7).

4.2 Optimized Geometries for the Entities Involved in the Acid-Catalyzed Hydrolysis in Gabapentin ProD1- ProD4

4.2.1 Global Minimum Geometries (GM)

The calculated B3LYP/6-31 G (d,p) geometries along with selected bond distances for the global minimum structures of Gabapentin **ProD1GM-ProD4GM** are illustrated in Figure7.

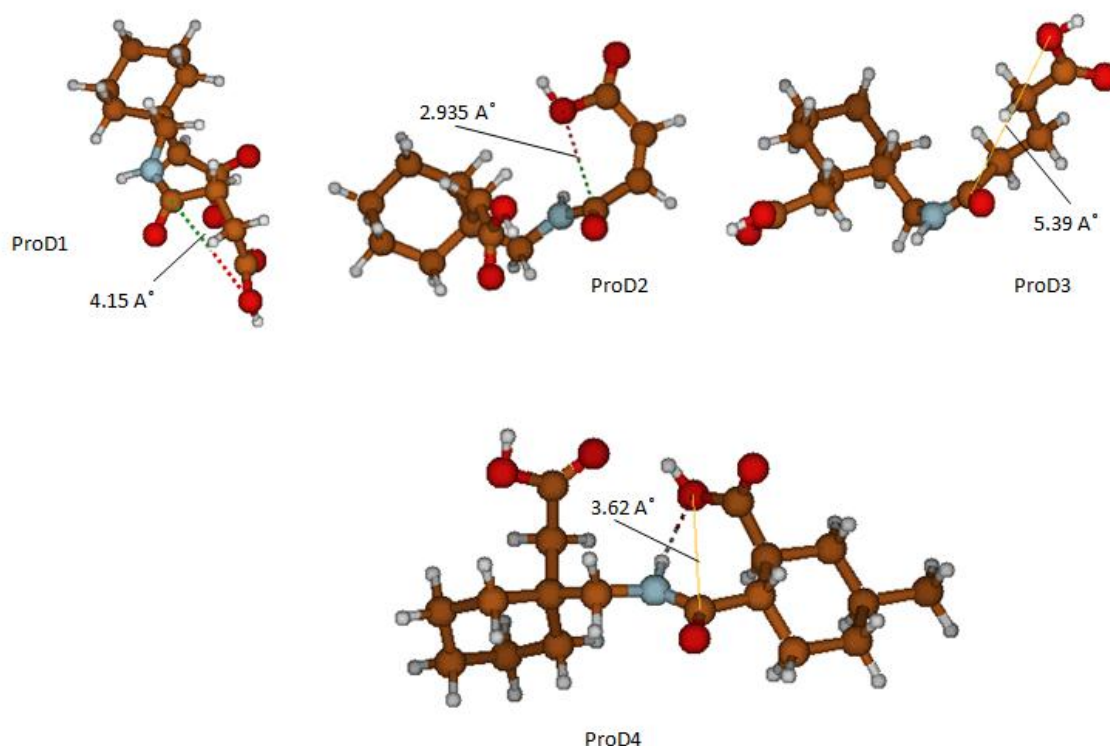


Figure 7: DFT optimized structures for the global minimum (GM) structures in Gabapentin **ProD1-ProD4**.

Inspection of the optimized structures for Gabapentin **ProD1GM-ProD4GM** indicates that the calculated DFT values for the intermolecular distance (r_{GM}) values were in the range of 2.93Å – 5.39Å (Figure 7) where the global minimum for **ProD2** having the shortest distance (2.93Å) and for **ProD3** the longest distance (5.39Å).

4.4.2 Transition State Geometries (TS):

The calculated properties for the transition state geometries of Gabapentin **ProD1-ProD4** (**ProD1TS-ProD4TS**) are summarized in Table 1 and illustrated in Figure 8.

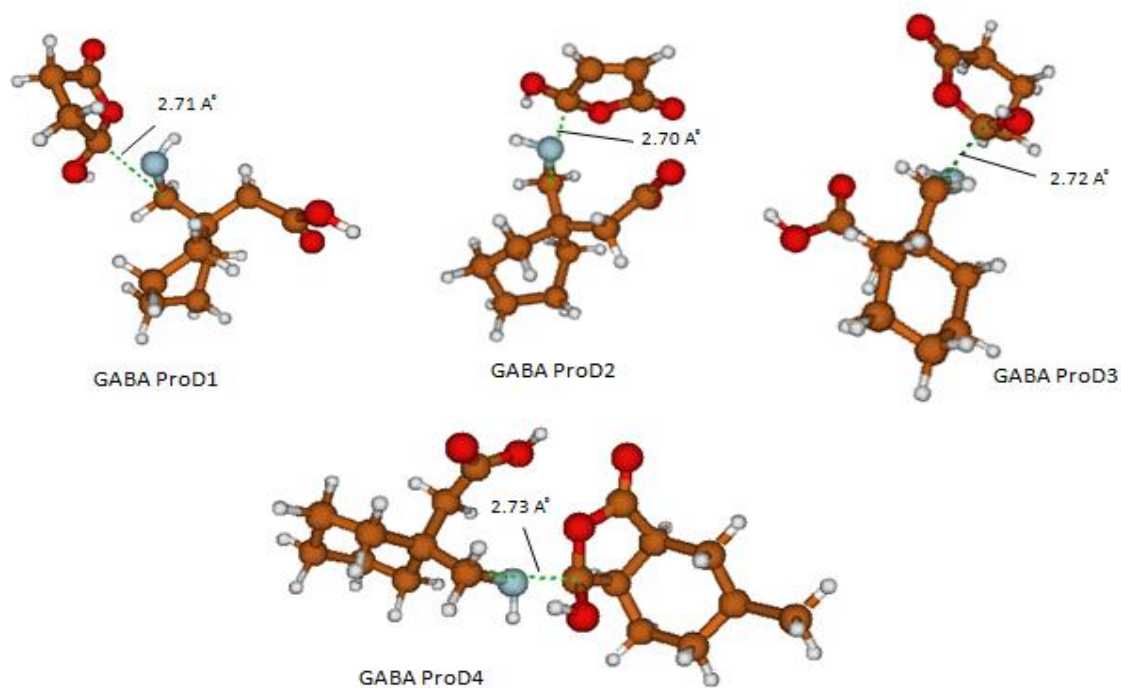


Figure 8: DFT optimized structures for the transition state (TS) structures in the intramolecular proton transfer reaction of Gabapentin **ProD1-ProD 4**.

Table 1: DFT (B3LYP) calculated properties of transition states and ground states for the proton transfer reactions in Gabapentin **ProD1-ProD4** in gas phase.

System	B3LYP, Enthalpy, H (gas phase) in Hartree	B3LYP, Entropy, S (gas phase) in Cal/Mol- Kelvin	B3LYP Frequency in Cm^{-1}
Gabapentin ProD1GM	-939.0046604	140.187	-----
Gabapentin ProD1TS	-938.9213672	149.181	411.75i
Gabapentin ProD2GM	-937.7590039	144.990	-----
Gabapentin ProD2TS	-937.6888698	135.455	402.36i
Gabapentin ProD3GM	-978.3125683	161.378	-----
Gabapentin ProD3TS	-978.245955	142.798	455.27i
Gabapentin ProD4GM	-1134.3792463	165.286	-----
Gabapentin ProD4TS	-1134.3114699	158.008	465.39i

B3LYP refer to values calculated by B3LYP/6-31G (d, p). (GM) and (TS) are global minimum and transition state structures, respectively.

I has calculated the enthalpy activation energies (ΔH^\ddagger), entropy activation energies ($T\Delta S^\ddagger$), and the free activation energies in the gas phase and water phase (ΔG^\ddagger) for the proton transfer reaction in these processes. The calculated energies are listed in Table 2.

Table 2: DFT (B3LYP) calculated properties of transition states and ground states for the proton transfer reactions in Gabapentin ProD1-ProD4 in water phase.

System	B3LYP, Enthalpy, H (water phase) in Hartree	B3LYP, Entropy, S (water phase) in Cal/Mol-Kelvin	B3LYP Frequency in Cm^{-1}
Gabapentin ProD1GM	-939.0529642	140.187	-----
Gabapentin ProD1TS	-939.0203507	149.181	411.75i
Gabapentin ProD2GM	-937.8157879	144.990	-----
Gabapentin ProD2TS	-937.7751217	135.455	402.36i
Gabapentin ProD3GM	-978.3768682	161.378	-----
Gabapentin ProD3TS	-978.3398305	142.798	455.27i
Gabapentin ProD4GM	-1134.4264284	165.286	-----
Gabapentin ProD4TS	-1134.4018707	158.008	465.39i

Table 3: DFT (B3LYP/6-31G (d,p) calculated kinetic and thermodynamic properties for the proton transfer in Gabapentin **ProD1-ProD4**.

System	ΔH^\ddagger (GP)	$T\Delta S^\ddagger$ (GP)	ΔG^\ddagger (GP)	ΔH^\ddagger (H_2O)	ΔG^\ddagger (H_2O)
Gabapentin ProD1	52.27	2.85	49.42	20.47	17.61
Gabapentin ProD2	44.01	-2.84	46.85	25.52	28.36
Gabapentin ProD3	41.80	-5.54	47.34	23.24	28.78
Gabapentin ProD4	42.53	-2.17	44.70	15.41	17.58

ΔH^\ddagger is the activation enthalpy energy (kcal/mol). $T\Delta S^\ddagger$ is the activation entropy energy in kcal/mol. ΔG^\ddagger is the activation free energy (kcal/mol).

4.3 The role of the strain energy of the intermediates (E_{sINT}) on the rate of the proton transfer in processes Gabapentin ProD1-ProD4.

We calculated, using Allinger's MM2 method [104], the strain energy values for the intermediates (E_{sINT}) in process Gabapentin **ProD1-ProD4** to examine the role of the (E_{sINT}) on the rate of the proton transfer in process Gabapentin **ProD 1-ProD4**. The MM2 strain energies of the intermediates are listed in (Table 3). The calculated MM2 (E_{sINT}) values for the process Gabapentin **ProD1-ProD4** were examined for correlation with the calculated DFT activation free energies (ΔG^\ddagger), a good correlation was found between the strain energy (E_{sINT}) of the intermediates and the calculated activation energies in water ($R^2 = 0.775$) (Figure 9), whereas a random correlation was observed when the E_{sINT} was plotted against the activation energies in the gas phase ($R^2 = 0.1644$) (Figure 10).

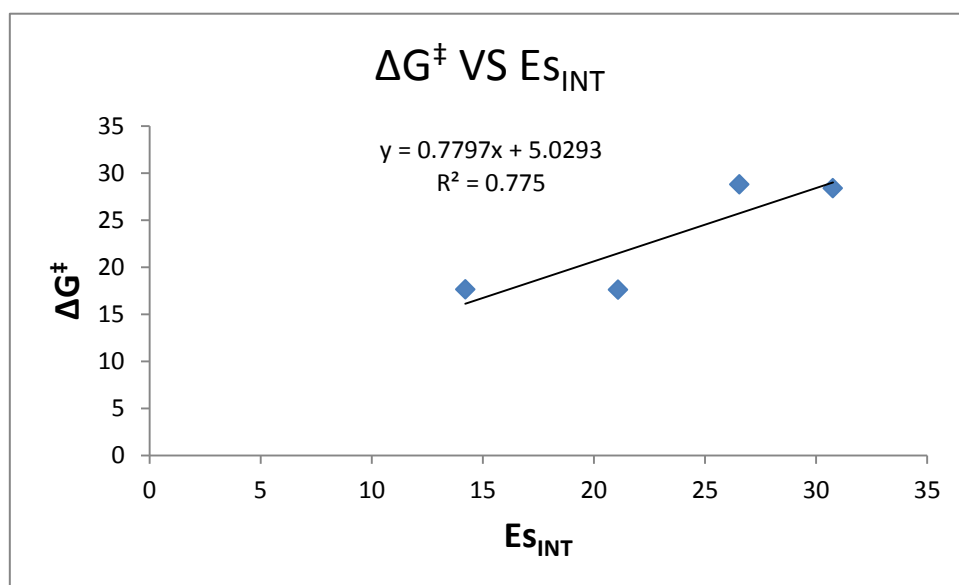


Figure 9: Plot of the DFT calculated ΔG^\ddagger vs. steric energy for intermediate in water phase for Gabapentin **ProD1-ProD4**

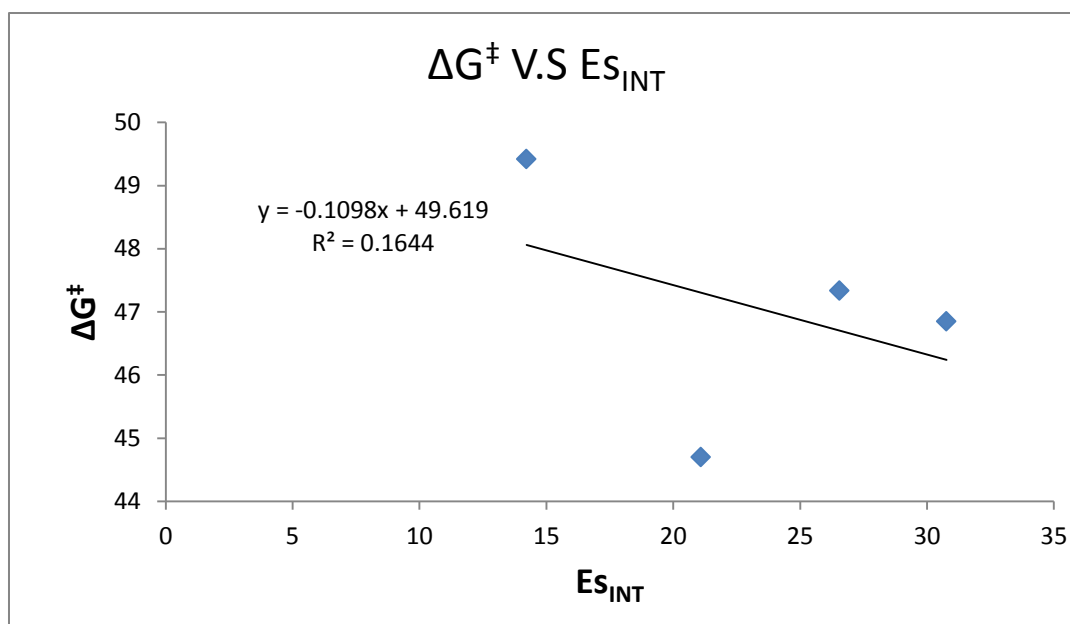


Figure 10: Plot of the DFT calculated ΔG^\ddagger vs. steric energy for intermediate in gas phase for Gabapentin **ProD1-ProD4**

Examination of Figure 10 and Table 3 reveals that the rate of a proton transfer in processes Gabapentin **ProD1-ProD4** is dependent on the strain energy of the tetrahedral intermediate. Systems having strained tetrahedral intermediates were found to be with low rates and vice versa. In order to further support this conclusion, the B3LYP 6-31G (d,p) activation energy values for **1-7** N-alkylmaleamic acid calculated in water (see Table 3) were examined for correlations with $\log k_{rel}$ (relative rate) and the results are shown in (Figure 11). A linear correlation was found between the activation free energy of **1-7** N-alkyl maleamic acid in water phase and $\log k_{rel}$ with a correlation coefficient of $R^2=0.9316$.

Table 4: DFT (B3LYP) calculated kinetic and thermodynamic properties for the acid-catalyzed hydrolysis of **1-7** N-alkylmaleamic acid and Gabapentin **ProD1- ProD4**.

System	E_{sINT}	ΔG^\ddagger	Log $k_{rel}[105]$
Gabapentin ProD1	14.216	17.61342	-
Gabapentin ProD2	30.763	28.3598	-
Gabapentin ProD3	26.5489	28.778	-
Gabapentin ProD4	21.0860	17.579	-
1	20.55	33.06	0
2	16.16	20.05	4.371
3	17.32	28.42	1.494
4	27.89	38.11	-4.377
5	19.25	23.12	2.732
6	17.59	27.28	1.516
7	18.55	27.55	1.648

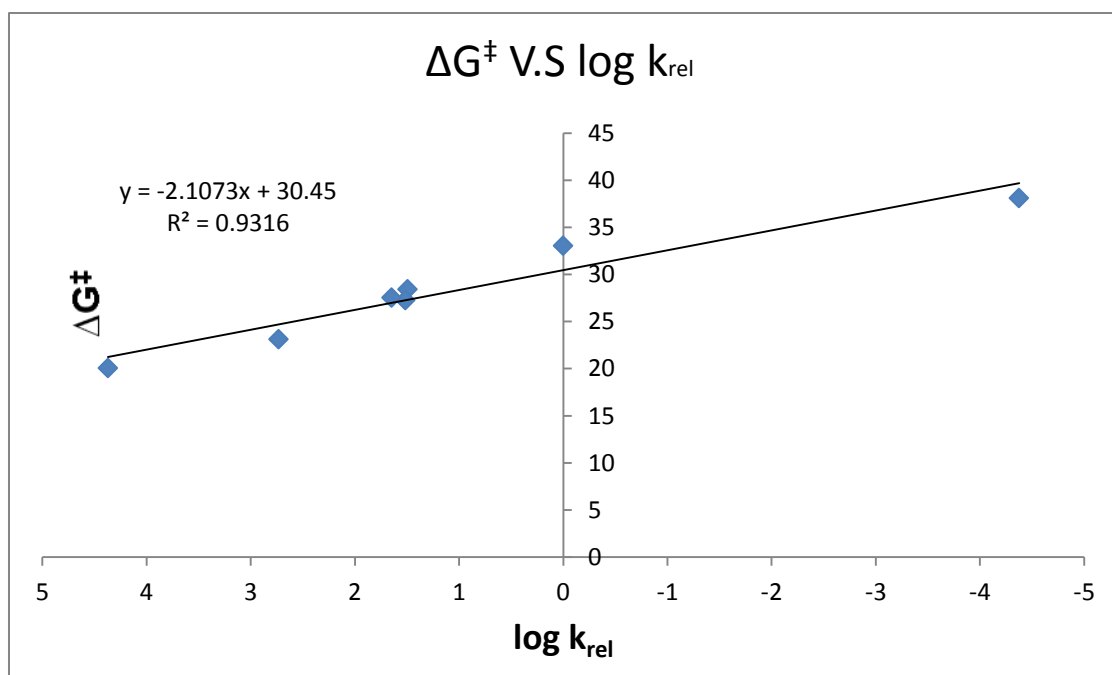


Figure 11: Plot of the DFT calculated ΔG^\ddagger vs. relative rate ($\log K_{rel}$) in **1-7** N-alkylmaleamic acid

Furthermore, a linear correlation was found between the strain energies for intermediates of **1-7** N-alkylmaleamic acid (E_{sINT}) and $\log k_{rel}$ (Figure 12) with a correlation coefficient of $R^2 = 0.8835$.

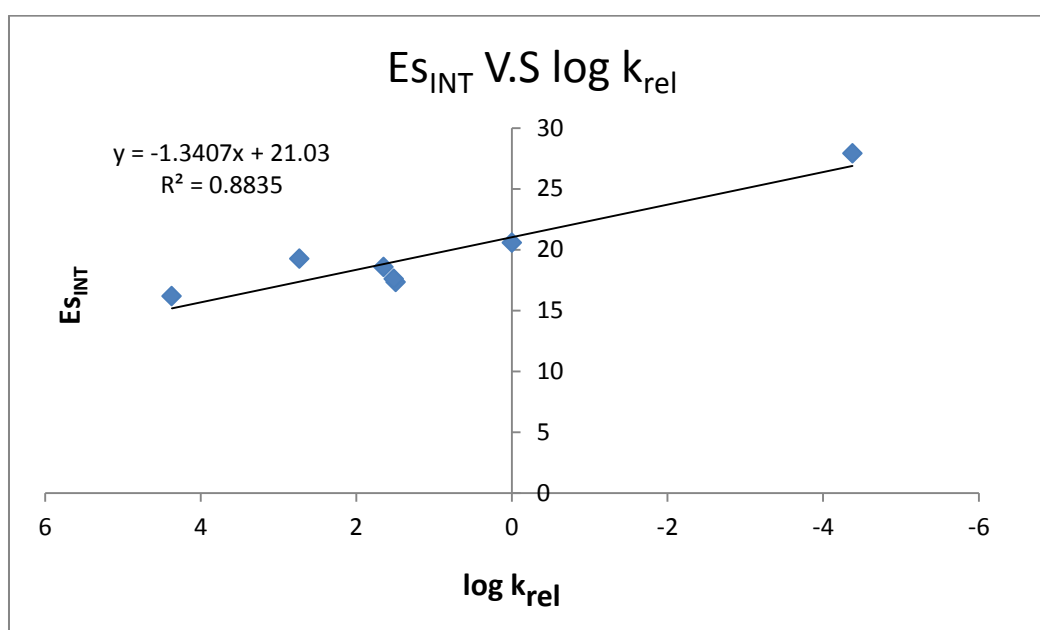


Figure 12: Plot of the steric energy for intermediates of **1-7-N-alkylmaleamic acid** vs. relative rate ($\log K_{rel}$)

Chapter Five
Conclusions and Future
Directions

Chapter 5

Conclusions and Future Directions

5.1 Conclusions

Based on the DFT calculations, results of Kirby`s enzyme model (proton transfer in *N*-alkylmaleamic acids), and novel Gabapentin prodrugs that can improve the bioavailability of the current medications to enhance effectiveness and to ease the use of the medications were designed.

The designed Gabapentin prodrugs have a carboxylic group as a hydrophilic moiety and a lipophilic moiety (hydrocarbon skeleton) where the combination of both groups ensures a modified hydrophilic-lipophilic balance value.

The DFT calculation results revealed that the rate of a proton transfer in processes of Gabapentin **ProD1-ProD4** and **1-7** is governed by strain effect of the tetrahedral intermediate. Systems, having strained tetrahedral intermediates, were found to be with low rates and vice versa.

Therefore, it is expected that the best candidates to fulfill the requirements needed to reach better bioavailability than the parent Gabapentin are Gabapentin **ProD1** and **ProD4**.

5.2 Future Directions

Based on the DFT calculations made for systems **1-7** and the designed Gabapentin prodrugs, it is recommended to synthesize Gabapentin **ProD1** and **ProD4** using Kirby`s synthetic procedure. *In vitro*, kinetic studies at different pH values should be made in order to be utilized for the *in vivo* pharmacokinetic studies which should be followed to determine the $t_{1/2}$ values for the conversion of the Gabapentin **ProD1** and **ProD4** to its parent drug, Gabapentin

References

1. Pauletti, G.M., et al., *Improvement of oral peptide bioavailability: Peptidomimetics and prodrug strategies*. *Advanced drug delivery reviews*, 1997. **27**(2-3): p. 235-256.
2. Stella, V.J., *A case for prodrugs*, in *Prodrugs*. 2007, Springer. p. 3-33.
3. Stella, V.J., W. Charman, and V. Naringrekar, *Prodrugs*. *Drugs*, 1985. **29**(5): p. 455-473.
4. Stella, V.J. and K.J. Himmelstein, *Prodrugs and site-specific drug delivery*. *Journal of medicinal chemistry*, 1980. **23**(12): p. 1275-1282.
5. Karaman, R., *Prodrugs for Masking the Bitter Taste of Drugs*, in *Application of Nanotechnology in Drug Delivery*. 2014, InTech.
6. Ueda, Y., et al., *Novel water soluble phosphate prodrugs of Taxol® possessing in vivo antitumor activity*. *Bioorganic & medicinal chemistry letters*, 1993. **3**(8): p. 1761-1766.
7. Karaman, R., *Prodrugs Design Based on Inter-and Intramolecular Chemical Processes*. *Chemical biology & drug design*, 2013. **82**(6): p. 643-668.
8. Kirby, A.J., *Efficiency of proton transfer catalysis in models and enzymes*. *Accounts of chemical research*, 1997. **30**(7): p. 290-296.
9. Karaman, R., *Reevaluation of Bruice's proximity orientation*. *Tetrahedron Letters*, 2009. **50**(4): p. 452-456.
10. Young, D., *Computational chemistry: a practical guide for applying techniques to real world problems*. 2004: John Wiley & Sons.
11. Amly, W. and R. Karaman, *Antibody Directed Enzyme Prodrug Therapy (ADEPT): A Promising Cancer Therapy Approach*. *PRODRUGS DESIGN*, 2014: p. 233.
12. Hejaz, H., R. Karaman, and M. Khamis, *Computer-assisted design for paracetamol masking bitter taste prodrugs*. *Journal of molecular modeling*, 2012. **18**(1): p. 103-114.
13. Karaman, R., D. Karaman, and I. Zeiadeh, *Computationally-designed phenylephrine prodrugs—a model for enhancing bioavailability*. *Molecular Physics*, 2013. **111**(21): p. 3249-3264.
14. Parr, R.G., *On the genesis of a theory*. *International Journal of Quantum Chemistry*, 1990. **37**(4): p. 327-347.

15. Chen, T.C., *Expansion of Electronic Wave Functions of Molecules in Terms of "United-Atom" Wave Functions*. The Journal of Chemical Physics, 1955. **23**(11): p. 2200-2201.
16. Parr, R.G. and W. Yang, *Density-Functional Theory of Atoms and Molecules*, vol. 16 of *International series of monographs on chemistry*. 1989, Oxford University Press, New York.
17. Dewar, M.J., et al., *Development and use of quantum mechanical molecular models. 76. AM1: a new general purpose quantum mechanical molecular model.*[Erratum to document cited in CA103 (2): 11627f]. Journal of the American Chemical Society, 1993. **115**(12): p. 5348-5348.
18. Dewar, M.J., C. Jie, and J. Yu, *SAM1; the first of a new series of general purpose quantum mechanical molecular models*. Tetrahedron, 1993. **49**(23): p. 5003-5038.
19. Younkin, J.M., L.J. Smith, and R.N. Compton, *Semi-empirical calculations of π -electron affinities for some conjugated organic molecules*. Theoretica chimica acta, 1976. **41**(2): p. 157-176.
20. Dewar, M.J. and W. Thiel, *Ground states of molecules. 38. The MNDO method. Approximations and parameters*. Journal of the American Chemical Society, 1977. **99**(15): p. 4899-4907.
21. Pople, J.A., P.M. Gill, and B.G. Johnson, *Kohn—Sham density-functional theory within a finite basis set*. Chemical physics letters, 1992. **199**(6): p. 557-560.
22. Gao, J., *Methods and applications of combined quantum mechanical and molecular mechanical potentials*. Reviews in computational chemistry, 1996: p. 119-185.
23. McLean, M.J., *Gabapentin in the management of convulsive disorders*. Epilepsia, 1999. **40**(s6): p. s39-s50.
24. Rowbotham, M., et al., *Gabapentin for the treatment of postherpetic neuralgia: a randomized controlled trial*. Jama, 1998. **280**(21): p. 1837-1842.
25. Rice, A., S. Maton, and P.N.S. Group1UK, *Gabapentin in postherpetic neuralgia: a randomised, double blind, placebo controlled study*. Pain, 2001. **94**(2): p. 215-224.
26. Sills, G.J., *The mechanisms of action of gabapentin and pregabalin*. Current opinion in pharmacology, 2006. **6**(1): p. 108-113.
27. Cundy, K.C., et al., *Clinical pharmacokinetics of XP13512, a novel transported prodrug of gabapentin*. J Clin Pharmacol, 2008. **48**(12): p. 1378-88.

28. Gordi, T., et al., *Pharmacokinetics of gabapentin after a single day and at steady state following the administration of gastric-retentive- extended-release and immediate-release tablets: a randomized, open-label, multiple-dose, three-way crossover, exploratory study in healthy subjects*. Clin Ther, 2008. **30**(5): p. 909-16.
29. Berry, D.J., et al., *The absorption of gabapentin following high dose escalation*. Seizure : the journal of the British Epilepsy Association, 2003. **12**(1): p. 28-36.
30. Taylor, C.P., et al., *A summary of mechanistic hypotheses of gabapentin pharmacology*. Epilepsy research, 1998. **29**(3): p. 233-249.
31. Lieberman, H. and N.M. Vemuri, *Chemical and Physicochemical Approaches to Solve Formulation Problems*, in *The Practice of Medicinal Chemistry*. 2015, Elsevier. p. 767-791.
32. Gidal, B.E., et al., *Inter-and intra-subject variability in gabapentin absorption and absolute bioavailability*. Epilepsy research, 2000. **40**(2): p. 123-127.
33. Agarwal, P., et al., *Gabapentin enacarbil-clinical efficacy in restless legs syndrome*. Neuropsychiatr Dis Treat, 2010. **6**: p. 151-158.
34. Najjar, A. and R. Karaman, *The prodrug approach in the era of drug design*. 2019, Taylor & Francis.
35. Svensson, L.-å. and A. Tunek, *The design and bioactivation of presystemically stable prodrugs*. Drug metabolism reviews, 1988. **19**(2): p. 165-194.
36. Ezra, A., et al., *A peptide prodrug approach for improving bisphosphonate oral absorption*. Journal of medicinal chemistry, 2000. **43**(20): p. 3641-3652.
37. Gangwar, S., et al., *Prodrug strategies to enhance the intestinal absorption of peptides*. Drug Discovery Today, 1997. **2**(4): p. 148-155.
38. Lal, R., et al., *Arbaclofen placarbil, a novel R-baclofen prodrug: improved absorption, distribution, metabolism, and elimination properties compared with R-baclofen*. Journal of Pharmacology and Experimental Therapeutics, 2009. **330**(3): p. 911-921.
39. Liu, Y., et al., *Covalently mucoadhesive amphiphilic prodrug of 5-fluorouracil for enhanced permeation and improved oral absorption*. Drug delivery and translational research, 2018. **8**(3): p. 645-656.
40. Markovic, M., et al., *Lipidic prodrug approach for improved oral drug delivery and therapy*. Medicinal research reviews, 2018.
41. Stappaerts, J., et al., *Rapid conversion of the ester prodrug abiraterone acetate results in intestinal supersaturation and enhanced absorption of abiraterone: in*

- vitro, rat in situ and human in vivo studies*. European Journal of Pharmaceutics and Biopharmaceutics, 2015. **90**: p. 1-7.
42. Senter, P.D., *Activation of prodrugs by antibody-enzyme conjugates: a new approach to cancer therapy*. The FASEB Journal, 1990. **4**(2): p. 188-193.
 43. Landowski, C.P., et al., *Floxuridine amino acid ester prodrugs: enhancing Caco-2 permeability and resistance to glycosidic bond metabolism*. Pharmaceutical research, 2005. **22**(9): p. 1510-1518.
 44. Rádl, S. (2014). Utilization of metabolic transformations in drug development; prodrugs, soft drugs, *Advances in Drug Discovery – Chemistry and Biology* 44.
 45. Nagasawa, H.T., et al., *N1-Alkyl-substituted derivatives of chlorpropamide as inhibitors of aldehyde dehydrogenase*. Journal of medicinal chemistry, 1989. **32**(6): p. 1335-1340.
 46. Blomberg, M., et al., *Orotidine Monophosphate Decarboxylase: A Mechanistic Dialogue*. Vol. 238. 2004: Springer Science & Business Media.
 47. Hanson, K.R. and E.A. Havir, *3 The Enzymic Elimination of Ammonia*. The enzymes, 1972. **7**: p. 75-166.
 48. Czarink, A.(1988) Intramolecularity: proximity and strain. Mechanistic principles of enzyme activity,.
 49. Sweigers, G., *Mechanical Catalysis*. Hoboken, NJ: John Wiley & Sons, 2008.
 50. Fersht, A., *Structure and mechanism in protein sciences: a guide to enzyme catalysis and protein folding*. W. H Freeman and Company, 1999.
 51. Nelson, D.L. and M.M. Cox, *Lehninger Principles of Biochemistry*. Worth Publishers. New York 2000.
 52. Page, M.I. (1983). The chemistry of enzyme action. *Elsevier*. Vol. 6.
 53. Dafforn, A. and D. Koshland Jr, *Proximity, entropy and orbital steering*. Biochemical and biophysical research communications, 1973. **52**(3): p. 779-785.
 54. Lightstone, F.C. and T.C. Bruice, *Separation of ground state and transition state effects in intramolecular and enzymatic reactions. 2. A theoretical study of the formation of transition states in cyclic anhydride formation*. Journal of the American Chemical Society, 1997. **119**(39): p. 9103-9113.
 55. Bruice, T.C. and U.K. Pandit, *The effect of geminal substitution ring size and rotamer distribution on the intramolecular nucleophilic catalysis of the hydrolysis of monophenyl esters of dibasic acids and the solvolysis of the intermediate*

- anhydrides*. Journal of the American Chemical Society, 1960. **82**(22): p. 5858-5865.
56. Bruice, T.C. and U.K. Pandit, *Intramolecular models depicting the kinetic importance of "Fit" in enzymatic catalysis*. Proceedings of the National Academy of Sciences, 1960. **46**(4): p. 402-404.
57. Milstien, S. and L.A. Cohen, *Concurrent general-acid and general-base catalysis of esterification*. Journal of the American Chemical Society, 1970. **92**(14): p. 4377-4382.
58. Milstien, S. and L.A. Cohen, *Rate acceleration by stereopopulation control: models for enzyme action*. Proceedings of the National Academy of Sciences, 1970. **67**(3): p. 1143-1147.
59. Milstien, S. and L.A. Cohen, *Stereopopulation control. I. Rate enhancement in the lactonizations of o-hydroxyhydrocinnamic acids*. Journal of the American Chemical Society, 1972. **94**(26): p. 9158-9165.
60. Menger, F. and M. Ladika, *Fast hydrolysis of an aliphatic amide at neutral pH and ambient temperature. A peptidase model*. Journal of the American Chemical Society, 1988. **110**(20): p. 6794-6796.
61. Menger, F., *On the source of intramolecular and enzymatic reactivity*. Accounts of chemical Research, 1985. **18**(5): p. 128-134.
62. Menger, F., et al., *Directionality of proton transfer in solution. Three systems of known angularity*. Journal of the American Chemical Society, 1983. **105**(15): p. 4996-5002.
63. Menger, F.M., A.L. Galloway, and D.G. Musaev, *Relationship between rate and distance*. Chemical Communications, 2003(18): p. 2370-2371.
64. Menger, F.M., *An alternative view of enzyme catalysis*. Pure and applied chemistry, 2005. **77**(11): p. 1873-1886.
65. Kirby, A.J. and F. Hollfelder, *From enzyme models to model enzymes*. 2009: Royal Society of Chemistry.
66. Barber, S.E., K.E. Dean, and A.J. Kirby, *A mechanism for efficient proton-transfer catalysis. Intramolecular general acid catalysis of the hydrolysis of 1-arylethyl ethers of salicylic acid*. Canadian journal of chemistry, 1999. **77**(5-6): p. 792-801.
67. Kirby, A. and P. Lancaster, *Structure and efficiency in intramolecular and enzymic catalysis. Catalysis of amide hydrolysis by the carboxy-group of substituted maleamic acids*. J. Chem. Soc., Perkin Trans. 2, 1972(9): p. 1206-1214.

68. Kirby, A.J., et al., *Efficient intramolecular general acid catalysis of nucleophilic attack on a phosphodiester*. Journal of the American Chemical Society, 2006. **128**(51): p. 16944-16952.
69. Kirby, A.J. and N.H. Williams, *Efficient intramolecular general acid catalysis of enol ether hydrolysis. Hydrogen-bonding stabilisation of the transition state for proton transfer to carbon*. J. Chem. Soc., Perkin Trans. 2, 1994(4): p. 643-648.
70. Kirby, A.J. and N.H. Williams, *Efficient intramolecular general acid catalysis of vinyl ether hydrolysis by the neighbouring carboxylic acid group*. J. Chem. Soc., Chem. Commun., 1991(22): p. 1643-1644.
71. Kirby, A.J., *Enzyme mechanisms, models, and mimics*. Angewandte Chemie International Edition in English, 1996. **35**(7): p. 706-724.
72. Fife, T.H. and T.J. Przystas, *Intramolecular general acid catalysis in the hydrolysis of acetals with aliphatic alcohol leaving groups*. Journal of the American Chemical Society, 1979. **101**(5): p. 1202-1210.
73. Karaman, R., *Antimalarial Atovaquone Prodrugs Based on Enzyme Models-Molecular Orbital Calculations Approach*. Antimalarial Drug Research and Development, Banet, A C. & Brasier, P. Ed, 2013: p. 1-67.
74. Karaman, R., K. Dajani, and H. Hallak, *Computer-assisted design for atenolol prodrugs for the use in aqueous formulations*. Journal of molecular modeling, 2012. **18**(4): p. 1523-1540.
75. Karaman, R., et al., *Design, synthesis and in vitro kinetic study of tranexamic acid prodrugs for the treatment of bleeding conditions*. Journal of computer-aided molecular design, 2013. **27**(7): p. 615-635.
76. Karaman, R., *Prodrugs for masking bitter taste of antibacterial drugs—a computational approach*. Journal of molecular modeling, 2013. **19**(6): p. 2399-2412.
77. Karaman, R., et al., *Prodrugs of acyclovir—a computational approach*. Chemical biology & drug design, 2012. **79**(5): p. 819-834.
78. Karaman, R., *Computational-Aided Design for Dopamine Prodrugs Based on Novel Chemical Approach*. Chemical biology & drug design, 2011. **78**(5): p. 853-863.
79. Karaman, R. and H. Hallak, *Computer-Assisted Design of Pro-drugs for Antimalarial Atovaquone*. Chemical biology & drug design, 2010. **76**(4): p. 350-360.

80. Karaman, R., et al., *Computationally designed atovaquone prodrugs based on Bruice's enzyme model*. Current computer-aided drug design, 2014. **10**(1): p. 15-27.
81. Karaman, R., et al., *Computationally designed prodrugs of statins based on Kirby's enzyme model*. Journal of molecular modeling, 2013. **19**(9): p. 3969-3982.
82. Karaman, R., *Analysis of Menger's 'spatiotemporal hypothesis'*. Tetrahedron Letters, 2008. **49**(41): p. 5998-6002.
83. Karaman, R., *The effective molarity (EM) puzzle in proton transfer reactions*. Bioorganic chemistry, 2009. **37**(4): p. 106-110.
84. Karaman, R., *Cleavage of Menger's aliphatic amide: a model for peptidase enzyme solely explained by proximity orientation in intramolecular proton transfer*. Journal of Molecular Structure: THEOCHEM, 2009. **910**(1): p. 27-33.
85. Karaman, R., *A general equation correlating intramolecular rates with 'attack' parameters: distance and angle*. Tetrahedron Letters, 2010. **51**(39): p. 5185-5190.
86. Karaman, R. and S. Alfalah, *Multi Transition States for SN2 Reaction in Intramolecular Processes*. International Review of Biophysical Chemistry (IREBIC), 2010. **1**(1): p. 14-23.
87. Karaman, R., B. Fattash, and A. Qtait, *The future of prodrugs—design by quantum mechanics methods*. Expert opinion on drug delivery, 2013. **10**(5): p. 713-729.
88. Kraut, D.A., K.S. Carroll, and D. Herschlag, *Challenges in enzyme mechanism and energetics*. Annual review of biochemistry, 2003. **72**(1): p. 517-571.
89. Kallarakal, A.T., et al., *Mechanism of the reaction catalyzed by mandelate racemase: structure and mechanistic properties of the K166R mutant*. Biochemistry, 1995. **34**(9): p. 2788-2797.
90. Karaman, R., *The role of proximity orientation in intramolecular proton transfer reactions*. Computational and Theoretical Chemistry, 2011. **966**(1-3): p. 311-321.
91. Katagi, T., *AMI study of acid-catalyzed hydrolysis of maleamic (4-amino-4-oxo-2-butenic) acids*. Journal of computational chemistry, 1990. **11**(9): p. 1094-1100.
92. Kluger, R. and J. Chin, *Carboxylic acid participation in amide hydrolysis. Evidence that separation of a nonbonded complex can be rate determining*. Journal of the American Chemical Society, 1982. **104**(10): p. 2891-2897.
93. Karaman, R., *Analyzing the efficiency in intramolecular amide hydrolysis of Kirby's N-alkylmaleamic acids—A computational approach*. Computational and Theoretical Chemistry, 2011. **974**(1-3): p. 133-142.

94. Oda, A. and O. Takahashi, *Validation of ArgusLab efficiencies for binding free energy calculations*. Chem-Bio Informatics Journal, 2009. **9**: p. 52-61.
95. Gaussian 09, R.A., Frisch MJ, Trucks GW, Schlegel H B, Scuseria GE, Robb MA, Cheeseman JR, Scalmani G, Barone V, Mennucci B, Petersson GA, Nakatsuji H, Caricato M, Li X, Hratchian, H, Izmaylov A F, Bloino J, Zheng G, Sonnenberg JL, Hada M, Ehara M, Toyota K, Fukuda R, Hasegawa J, Ishida M, Nakajima T, Honda Y, Kitao O, Nakai H, Vreven T, Montgomery Jr. JA, Peralta JE, Ogliaro F, Bearpark M, Heyd JJ, Brothers E, Kudin KN, Staroverov VN, Kobayashi R, Noemand J, Raghavachari K, Rendell A, Burant JC, Iyengar SS, Tomasi J, Cossi M, Rega N, Millam JM, Klene M, Knox JE, Cross JB, Bakken V, Adamo C, Jaramillo J, Gomperts R, Stratmann RE, Yazyev O, Austin AJ, Cammi R, Pomelli C, Ochterski JW, Martin RL, Morokuma K, Zakrzewski VG, Voth GA, Salvador P, Dannenberg JJ, Dapprich S, Daniels AD, Farkas O, Foresman JB, Ortiz JV, Cioslowski J, Fox DJ Gaussian, Inc., Wallingford CT, 2009
96. Casewit, C., Colwell KS, Rappe AK (1992) Application of a universal force field to main group compounds. J Am Chem Soc 114:10046-10053.
97. Müller, K., *Reaction paths on multidimensional energy hypersurfaces*. Angewandte Chemie International Edition in English, 1980. **19**(1): p. 1-13.
98. Cancès MT, Mennucci B, and T. J, *A new integral equation formalism for the polarizable continuum model: Theoretical background and applications to isotropic and anisotropic dielectrics*. J Chem Phys, 1997. **107**(8): p. 3032-3041.
99. Mennucci B and T. J, *Continuum solvation models: A new approach to the problem of solute's charge distribution and cavity boundaries*. J Chem Phys, 1997. **106**: p. 5151.
100. Mennucci, B., E. Cancès, and J. Tomasi, *Evaluation of solvent effects in isotropic and anisotropic dielectrics and in ionic solutions with a unified integral equation method: theoretical bases, computational implementation, and numerical applications*. The Journal of Physical Chemistry B, 1997. **101**(49): p. 10506-10517.
101. Mennucci B, C. MT, and T. J, *Evaluation of solvent effects in isotropic and anisotropic dielectrics and in ionic solutions with a unified integral equation method: theoretical bases, computational implementation, and numerical applications*. The Journal of Physical Chemistry B, 1997. **101**(49): p. 10506-10517.

102. Tomasi J, M.B., Cancès MT(1997) The IEF version of the PCM solvation method: an overview of a new method addressed to study molecular solutes at the QM ab initio level . *J Mol Struct.(Theochem)* 464:211-226.
103. Kirby, A.J. and N.H. Williams, *Efficient intramolecular general acid catalysis of enol ether hydrolysis. Hydrogen-bonding stabilisation of the transition state for proton transfer to carbon*. *Journal of the Chemical Society, Perkin Transactions 2*, 1994(4): p. 643-648.
104. Lipkowitz, K., *Molecular mechanics*, by Ulrich Burkert and Norman L. Allinger, published by the American Chemical Society, 1982. 339 pages, \$64.95. *Journal of Computational Chemistry*, 1983. 4(4): p. 605-605.
105. Kirby, A. and P. Lancaster, *Structure and efficiency in intramolecular and enzymic catalysis. Catalysis of amide hydrolysis by the carboxy-group of substituted maleamic acids*. *Journal of the Chemical Society, Perkin Transactions 2*, 1972(9): p. 1206-1214.

Supplementary Material

Supplementary Material

*XYZ Cartesian coordinates for the DFT optimized GM, TS and P in processes
Gabapentin ProD1-ProD4.*

Gabapentin ProD1GM

C	0.000000	0.000000	0.000000
C	0.000000	0.000000	1.536890
C	1.416582	0.000000	2.170914
C	2.250449	-1.144128	1.536401
C	2.277365	-1.110648	0.000065
C	0.854989	-1.137305	-0.576591
C	1.226212	-0.274789	3.690979
N	2.419556	-0.060555	4.498153
C	2.576747	0.681668	5.637757
O	3.670152	0.761277	6.190541
C	2.152706	1.354836	1.933447
C	1.751971	2.455856	2.895688
O	0.601983	2.716920	3.209444
C	1.345791	1.385299	6.214963
C	1.726674	2.233201	7.425233
C	2.537710	3.458095	7.069192
O	2.572503	4.020596	5.988491
O	3.204568	3.942264	8.132311
O	2.816565	3.092396	3.398354

H	-0.556132	0.862744	1.916717
H	-0.527728	-0.900475	1.884116
H	1.812309	-2.101500	1.852763
H	3.276662	-1.126305	1.927368
H	2.800987	-0.210648	-0.348724
H	2.856394	-1.963535	-0.373052
H	0.387982	-2.101928	-0.330919
H	0.885068	-1.075683	-1.670740
H	-1.032307	-0.079994	-0.360140
H	0.373964	0.961549	-0.376919
H	0.440504	0.379915	4.065521
H	0.870041	-1.308458	3.807373
H	3.274719	-0.526018	4.221162
H	0.614423	0.626392	6.518294
H	0.858597	2.004998	5.456799
H	0.821271	2.596228	7.928553
H	2.294954	1.652223	8.153511
H	3.675480	4.735842	7.825164
H	3.233968	1.221071	2.008316
H	1.947504	1.710842	0.918550
H	2.534813	3.643424	4.161950

Gabapentin ProD2 GM

C	0.000000	0.000000	0.000000
C	0.000000	0.000000	1.536391
C	1.422070	0.000000	2.158861
C	2.227043	-1.176019	1.541908
C	2.231918	-1.196916	0.004188
C	0.807533	-1.175577	-0.567014
C	1.264223	-0.228826	3.686336
N	2.507935	-0.415633	4.429705
C	3.122511	0.581108	5.117465
O	2.726820	1.741348	5.162532
C	2.186226	1.322397	1.906925
C	1.559284	2.594850	2.443197
O	2.431995	3.625371	2.350333
C	4.289630	0.178314	5.983440
C	5.542076	-0.176019	5.660065
C	6.152824	-0.325031	4.321412
O	7.311161	-0.645436	4.151895
O	5.318881	-0.063366	3.279756
O	0.433097	2.744615	2.869225
H	-0.566116	0.850977	1.920887
H	-0.515286	-0.909564	1.878733
H	1.776661	-2.115591	1.896255

H	3.256135	-1.160338	1.919387
H	2.792395	-0.335516	-0.382866
H	2.769250	-2.086945	-0.344962
H	0.302249	-2.116600	-0.306214
H	0.836967	-1.131123	-1.662168
H	-1.034267	-0.041757	-0.361233
H	0.411591	0.946007	-0.377148
H	0.746367	0.621936	4.132401
H	0.650441	-1.122995	3.845186
H	2.969221	-1.311873	4.392171
H	4.063780	0.294947	7.042073
H	6.260791	-0.357940	6.452791
H	5.860878	-0.161974	2.478929
H	2.335938	1.488177	0.833719
H	3.191678	1.257663	2.334276
H	1.975431	4.395248	2.729464

Gabapentin **ProD3GM**

C	0.000000	0.000000	0.000000
C	0.000000	0.000000	1.543674
C	1.452168	0.000000	2.090868
C	2.242215	-1.180313	1.484279
C	2.228702	-1.189167	-0.048485

C	0.794756	-1.171027	-0.588327
C	-0.855737	1.160631	2.075247
C	-2.330374	1.017283	1.754271
O	-2.980117	2.200256	1.873133
C	1.552879	-0.067036	3.638928
N	1.500639	1.205721	4.349736
C	2.533520	2.055547	4.651266
O	2.322523	3.096332	5.266853
C	3.936027	1.635349	4.210339
C	5.005469	2.684855	4.526674
C	4.863967	3.962116	3.697422
C	5.989066	4.940912	3.938334
O	6.926601	4.784299	4.690061
O	5.839289	6.065371	3.192080
O	-2.902114	-0.011469	1.464370
H	-0.479546	-0.932444	1.875343
H	1.937894	0.934161	1.770349
H	1.813318	-2.122630	1.856575
H	3.276710	-1.148209	1.849277
H	2.767572	-0.305579	-0.418840
H	2.772149	-2.064635	-0.422783
H	0.294313	-2.114175	-0.328870
H	0.797720	-1.111226	-1.682870

H	-1.032544	-0.032684	-0.360296
H	0.433340	0.947894	-0.353371
H	2.488268	-0.567961	3.906874
H	0.751480	-0.702379	4.034040
H	0.614357	1.535025	4.707122
H	4.185681	0.695203	4.720241
H	3.929343	1.398561	3.138173
H	5.994584	2.248812	4.354307
H	4.955789	2.943086	5.587608
H	4.841450	3.744815	2.620823
H	3.918932	4.463783	3.928826
H	6.596019	6.633833	3.413825
H	-0.503517	2.128977	1.703309
H	-0.808147	1.230085	3.167793
H	-3.917699	2.013110	1.694871

Gabapentin **ProD4GM**

C	-2.389495	-1.676481	-0.837948
C	-2.577277	-0.455799	0.101371
C	-3.927409	-0.612699	0.850269
C	-5.128705	-0.862338	-0.074034
C	-4.894623	-2.070920	-0.991823
C	3.580517	-1.934546	-1.774376

C	-1.460369	-0.436958	1.168856
N	-0.112097	-0.352874	0.622711
C	0.958570	-0.830626	1.327698
O	0.822066	-1.517070	2.336073
C	-2.538687	0.847713	-0.771788
C	-2.508358	2.164677	-0.030327
O	-1.551399	2.916818	0.057418
C	2.380679	-0.495416	0.831035
C	2.544450	0.412299	-0.421286
C	4.043471	0.640712	-0.721348
C	4.827257	-0.668873	-0.900395
C	4.640207	-1.568215	0.331642
C	3.161483	-1.813937	0.645222
C	1.867076	1.757074	-0.202308
O	0.792581	1.916955	-1.023569
C	6.306616	-0.393083	-1.190879
O	2.199949	2.579269	0.619598
O	-3.689669	2.481139	0.538644
H	-4.113855	0.259397	1.483776
H	-3.826093	-1.473456	1.525176
H	-2.245447	-2.560059	-0.201441
H	-1.464520	-1.565201	-1.414263
H	-3.671888	-1.122242	-2.508221

H	-3.390109	-2.843542	-2.356829
H	-4.852186	-2.982334	-0.378955
H	-5.738122	-2.197684	-1.680499
H	-6.025224	-1.019186	0.536908
H	-5.332559	0.030600	-0.679805
H	-1.638067	0.394677	1.868919
H	-1.502604	-1.352463	1.763112
H	0.048345	0.316842	-0.116031
H	-3.414242	0.866383	-1.426267
H	-1.654809	0.834925	-1.413837
H	-3.560622	3.335991	0.985907
H	6.859300	-1.325687	-1.347161
H	6.777892	0.137031	-0.354786
H	6.430318	0.224020	-2.087514
H	0.220820	2.638990	-0.681992
H	4.140224	1.259439	-1.622096
H	4.473479	1.221478	0.104560
H	4.402413	-1.198297	-1.767840
H	5.122416	-1.091957	1.197764
H	5.152928	-2.525815	0.177721
H	2.701849	-2.388630	-0.171717
H	3.043095	-2.407598	1.554860
H	2.831091	0.045721	1.674263

H 2.076419 -0.073620 -1.285475

Gabapentin ProD1TS

C	0.000000	0.000000	0.000000
N	0.000000	0.000000	1.842000
C	1.328161	0.000000	2.356866
O	2.109162	-1.149474	1.866678
O	2.037957	1.158608	2.006044
C	2.954546	-1.617103	2.839154
O	3.736286	-2.507807	2.636537
C	2.715951	-0.836489	4.126332
C	1.373774	-0.142815	3.888606
C	-1.306123	0.597411	-0.509003
C	-2.464884	-0.336816	-0.044078
C	-1.514066	2.024074	0.049497
C	-0.417570	3.019458	-0.378276
C	-1.206278	0.632082	-2.080505
C	-1.047561	2.051523	-2.653209
O	-0.011867	2.866784	-1.869688
C	-4.288193	-0.017715	-1.620660
O	-3.837610	0.106837	-0.500608
H	-4.547259	0.687341	0.498080
H	-5.399312	0.946744	0.106534

H	-2.488182	2.389793	-0.294852
H	-0.789334	4.033298	-0.192773
H	-2.093342	0.162813	-2.512643
H	-2.015072	2.568148	-2.629383
H	0.125256	3.851109	-2.330326
H	-0.764972	1.984178	-3.709932
H	0.961301	2.362872	-1.949046
H	-0.348629	0.024013	-2.400373
H	0.456689	2.899393	0.270435
H	0.868017	0.603917	-0.248896
H	0.156639	-1.042250	-0.278132
H	-0.408179	-0.909553	2.057038
H	1.278423	0.837969	4.355266
H	0.541305	-0.768935	4.223281
H	2.746951	-1.509160	4.985236
H	3.531471	-0.113870	4.235484
H	2.449521	0.994558	1.146729
H	-2.302856	-1.338648	-0.456568
H	-2.461111	-0.395484	1.046377
H	-1.562623	1.973304	1.140144

Gabapentin ProD2TS

C	0.000000	0.000000	0.000000
---	----------	----------	----------

C	0.000000	0.000000	1.490709
O	1.340865	0.000000	1.886237
C	2.148453	0.147777	0.756693
C	1.261281	0.096374	-0.425250
N	-0.645044	1.664323	1.945585
C	0.155604	2.064972	3.270663
C	-0.015390	3.608093	3.397662
C	0.779484	3.903306	4.706215
C	0.391614	5.246095	5.338325
C	-1.084968	5.246968	5.798924
C	-1.960654	4.330785	4.912885
C	-1.420803	4.279150	3.478724
C	0.697745	4.201395	2.146535
C	1.832583	3.417218	1.517240
O	1.961065	3.239202	0.324402
O	-0.736752	-0.994764	2.064196
O	3.337692	0.300510	0.854309
O	2.728700	2.934503	2.415118
H	0.579679	3.105402	5.435243
H	1.851867	3.859050	4.498707
H	-2.112748	3.753101	2.810053
H	-1.360036	5.305106	3.091922
H	-1.978845	3.315756	5.329999

H	-3.000552	4.676035	4.917960
H	-1.474658	6.271562	5.775208
H	-1.152349	4.918084	6.842740
H	1.053382	5.473219	6.181397
H	0.553602	6.049424	4.607636
H	0.840583	1.640095	3.415188
H	-0.784437	1.703203	4.101108
H	-1.640312	1.443507	1.991214
H	1.088384	5.193889	2.409968
H	-0.021488	4.340737	1.338727
H	3.350925	2.371771	1.916543
H	-0.563090	-0.988690	3.017432
H	1.640154	0.180298	-1.433406
H	-0.911504	-0.032832	-0.581338

Gabapentin **ProD3TS**

C	0.000000	0.000000	0.000000
O	0.000000	0.000000	1.378591
C	1.190782	0.000000	2.147027
C	2.371215	-0.720958	1.546871
C	2.615915	-0.228636	0.117753
C	1.357738	-0.464554	-0.717210
N	0.742110	-0.961656	3.652642

C	-0.145955	-0.154604	4.488579
C	-0.278140	-0.727346	5.927644
C	-1.341819	0.104853	6.684836
C	-1.422125	-0.203118	8.189379
C	-0.053438	-0.074315	8.870996
C	1.006931	-0.927969	8.163196
C	1.080324	-0.603715	6.664590
C	-0.666278	-2.242042	5.860950
C	-1.890658	-2.529140	5.027671
O	-3.027002	-2.594815	5.766375
O	1.522593	1.283287	2.488708
O	-1.022292	0.267717	-0.572058
O	-1.904645	-2.679575	3.821545
H	-2.326845	-0.029198	6.223213
H	-1.083979	1.166493	6.559026
H	1.421450	0.435604	6.556280
H	1.826664	-1.222915	6.157216
H	0.782725	-1.992326	8.316187
H	1.991523	-0.763491	8.617924
H	0.261146	0.979006	8.846145
H	-0.126672	-0.352022	9.929310
H	-2.145590	0.474100	8.659006
H	-1.816755	-1.216155	8.340380

H	-1.152491	-0.026632	4.058857
H	0.293905	0.845781	4.593961
H	0.158648	-1.680203	3.215873
H	2.162905	-1.795512	1.556053
H	3.231892	-0.545206	2.194890
H	2.867686	0.837016	0.138494
H	3.463343	-0.753664	-0.333883
H	1.230253	-1.538909	-0.908105
H	1.391562	0.026930	-1.691880
H	-0.820991	-2.639880	6.865190
H	0.164043	-2.779266	5.397247
H	-3.748640	-2.757608	5.134320
H	0.699879	1.764218	2.664267

Gabapentin **ProD4TS**

C	-3.182805	-1.651532	-0.691873
C	-2.729744	-0.435819	0.158307
C	-3.775262	-0.189680	1.277876
C	-5.220916	-0.088969	0.765713
C	-5.618818	-1.310320	-0.074245
C	-4.622600	-1.544863	-1.218715
C	-1.375513	-0.764949	0.838326
N	-0.279160	-0.952367	-0.127030

C	1.017449	-0.459205	0.246649
C	2.055787	-0.611203	-0.891103
C	2.858205	0.704279	-0.799182
C	1.837384	1.670970	-0.223404
O	0.867105	0.967832	0.428632
C	2.904871	-1.894408	-0.920568
C	4.135376	-1.875855	-0.001455
C	4.971249	-0.595250	-0.171781
C	4.094693	0.631327	0.129113
O	1.818801	2.876822	-0.264609
O	1.546005	-0.993845	1.440659
C	6.220150	-0.613400	0.715852
C	-2.564205	0.798475	-0.773570
C	-1.881849	2.003911	-0.151006
O	-1.097350	2.637913	-1.048136
O	-2.006679	2.384721	0.995822
H	-3.504375	0.713582	1.830776
H	-3.717953	-1.030621	1.985173
H	-3.114204	-2.549726	-0.059813
H	-2.484918	-1.799179	-1.525364
H	-4.697815	-0.724590	-1.944950
H	-4.879448	-2.459134	-1.767229
H	-5.639053	-2.200478	0.571006

H	-6.634157	-1.189857	-0.470424
H	-5.899759	0.021942	1.619488
H	-5.343546	0.822425	0.165118
H	4.666521	1.559745	0.023205
H	3.765812	0.574202	1.173922
H	5.297969	-0.533909	-1.222475
H	3.816968	-1.955676	1.043373
H	4.754086	-2.755555	-0.218075
H	3.244584	-2.031608	-1.955413
H	2.276929	-2.763809	-0.691208
H	1.457478	-0.569714	-1.807114
H	3.169410	1.057404	-1.786576
H	-1.120332	0.073635	1.491805
H	-1.512651	-1.650451	1.477247
H	-0.194261	-1.921991	-0.413806
H	6.853804	-1.477396	0.488708
H	5.945227	-0.671864	1.775565
H	6.822263	0.290866	0.576944
H	-3.545305	1.136592	-1.125823
H	-1.990759	0.515262	-1.657771
H	-0.560910	3.290157	-0.560492
H	0.958734	-0.732274	2.164880

Gabapentin ProD1INT

O	0.000000	0.000000	0.000000
C	0.000000	0.000000	1.466375
C	1.495561	0.000000	1.922101
C	2.305355	0.051420	0.633372
C	1.289966	0.035577	-0.478149
N	-0.777972	-1.115920	1.985769
C	-2.212875	-0.992775	1.814098
C	-3.024237	-2.295807	2.025117
C	-4.514790	-1.910138	2.024654
C	-5.144115	-1.946443	3.405026
C	-4.236428	-1.365800	4.468895
C	-2.911928	-2.105570	4.551018
C	-2.654355	-2.980557	3.339628
C	-2.726464	-3.238537	0.850293
C	-3.458989	-4.541292	0.951724
O	-4.625000	-4.811433	0.656199
O	-0.527874	1.268564	1.759382
O	1.411760	0.043685	-1.694601
O	-2.698455	-5.574724	1.410152
H	-4.636300	-0.883297	1.591450
H	-5.084580	-2.611004	1.357966
H	-1.577757	-3.288827	3.323677

H	-3.259377	-3.923318	3.421587
H	-2.078100	-1.364318	4.657897
H	-2.895336	-2.753897	5.464954
H	-4.753949	-1.407535	5.461393
H	-4.050767	-0.283540	4.242727
H	-6.107015	-1.373465	3.379509
H	-5.396944	-3.005326	3.672586
H	-1.629500	-3.461684	0.799183
H	-3.038955	-2.747880	-0.109037
H	-3.228350	-6.386525	1.435535
H	-2.469095	-0.592823	0.789245
H	-2.561586	-0.242003	2.580148
H	-0.423798	-1.974804	1.615016
H	-1.351241	1.382406	1.265536
H	1.734786	-0.907686	2.523535
H	1.669281	0.902044	2.557624
H	2.991192	-0.825128	0.532602
H	2.918234	0.984269	0.564408

Gabapentin ProD2INT

C	0.000000	0.000000	0.000000
C	0.000000	0.000000	1.517662
O	1.331367	0.000000	2.066738

C	2.293378	0.755957	1.435984
C	2.019200	1.386177	0.103790
C	0.958961	0.667283	-0.645436
N	-0.750334	1.148220	2.044495
C	-0.765519	1.260987	3.487852
C	-1.534692	2.503104	4.004807
C	-1.272219	2.580947	5.514580
C	-2.155819	3.580119	6.234829
C	-3.624617	3.342199	5.946849
C	-3.885136	3.346791	4.453768
C	-3.033110	2.311149	3.746263
C	-1.054495	3.771737	3.294818
C	0.413839	3.799823	3.003139
O	1.235744	3.686540	4.082720
O	-0.472215	-1.259059	1.962767
O	3.335481	0.814021	2.084478
O	0.970685	3.955705	1.912304
H	-0.195902	2.849843	5.680304
H	-1.442500	1.563991	5.955629
H	-3.327229	1.289520	4.102836
H	-3.239908	2.358353	2.646139
H	-3.662993	4.363354	4.037400
H	-4.966869	3.131338	4.258775

H	-3.936765	2.356222	6.377953
H	-4.240129	4.136428	6.440709
H	-1.971276	3.497281	7.337237
H	-1.880326	4.623548	5.932499
H	-1.298073	4.669040	3.922871
H	-1.583913	3.877072	2.310287
H	2.162090	3.697358	3.793400
H	0.306160	1.340554	3.831721
H	-1.212880	0.345330	3.972695
H	-1.674811	1.142411	1.662888
H	2.977054	1.415809	-0.478866
H	1.696481	2.452760	0.293186
H	1.009492	0.718128	-1.742214
H	-0.802239	-0.574276	-0.475901
H	-0.056326	-1.463066	2.811130

Gabapentin ProD3INT

C	0.000000	0.000000	0.000000
O	0.000000	0.000000	1.366804
C	1.232638	0.000000	2.130596
C	2.475605	-0.472738	1.338458
C	2.494806	0.172604	-0.028718
C	1.249806	-0.207367	-0.797776

N	1.027530	-0.790031	3.346201
C	-0.188505	-0.499908	4.081247
C	-0.284631	-1.230104	5.446152
C	-1.674768	-0.915965	6.014610
C	-1.847619	-1.336267	7.461004
C	-0.747246	-0.789391	8.348073
C	0.619984	-1.166431	7.813265
C	0.799925	-0.693430	6.384184
C	-0.104709	-2.741517	5.273566
C	-0.806878	-3.276705	4.063958
O	-2.118862	-3.583500	4.241936
O	1.408012	1.379189	2.375000
O	-1.131490	0.152199	-0.460435
O	-0.337431	-3.496536	2.942533
H	-2.446253	-1.434353	5.386131
H	-1.849731	0.188430	5.933945
H	0.764210	0.426979	6.361600
H	1.808703	-1.002828	6.008750
H	0.749349	-2.278404	7.862323
H	1.414756	-0.707798	8.455794
H	-0.830796	0.326520	8.403515
H	-0.869468	-1.188578	9.387235
H	-2.840623	-0.967715	7.827711

H	-1.865640	-2.454469	7.533553
H	-1.106470	-0.769209	3.480709
H	-0.222837	0.607486	4.277552
H	1.083343	-1.765430	3.116708
H	2.455592	-1.587032	1.239592
H	3.385339	-0.178750	1.920068
H	2.548321	1.286800	0.087461
H	3.403643	-0.158038	-0.592623
H	1.284945	-1.291771	-1.087271
H	1.170466	0.393728	-1.740923
H	-0.494488	-3.270560	6.182393
H	0.985486	-2.985297	5.165093
H	-2.493793	-3.916829	3.411058
H	0.584863	1.741467	2.726782

Gabapentin **ProD4 INT**

C	-2.371717	1.546406	-1.127091
C	-3.190124	1.068449	0.056524
C	-2.198029	0.193807	0.842063
C	-1.097491	-0.167349	-0.222099
O	-1.214002	0.804651	-1.289088
C	-4.429974	0.358573	-0.469120
C	-5.007752	-0.613651	0.547022

C	-3.950075	-1.651631	0.893661
C	-2.766209	-1.000468	1.575997
C	-6.253182	-1.275114	-0.006337
N	0.254546	-0.158678	0.339649
C	1.313274	0.004180	-0.639099
C	2.730505	-0.325516	-0.108645
C	3.710035	0.031750	-1.234350
C	5.122430	-0.456334	-0.982462
C	5.157646	-1.944055	-0.695467
C	4.241684	-2.290705	0.460970
C	2.822119	-1.824143	0.202714
C	3.031030	0.469120	1.162493
C	2.742689	1.933266	1.053963
O	2.850606	2.711032	0.103030
O	-1.442998	-1.378802	-0.869695
O	-2.552752	2.424663	-1.955924
O	2.333708	2.486424	2.231986
H	3.715994	1.145801	-1.368898
H	3.335519	-0.424652	-2.187925
H	2.404370	-2.391605	-0.669413
H	2.195420	-2.068425	1.098909
H	4.628663	-1.817859	1.400542
H	4.239703	-3.399721	0.620537

H	4.837941	-2.509070	-1.608758
H	6.204791	-2.258194	-0.453457
H	5.748723	-0.233758	-1.884808
H	5.573409	0.102301	-0.122162
H	-5.196942	1.126878	-0.745036
H	-4.168485	-0.209052	-1.401342
H	-5.282792	-0.047867	1.479301
H	-3.607167	-2.166180	-0.041977
H	-4.387768	-2.427861	1.571442
H	-3.080296	-0.663620	2.600093
H	-1.952649	-1.761329	1.705684
H	-1.699447	0.856701	1.605182
H	-3.499012	1.945970	0.682099
H	1.294287	1.083511	-0.967335
H	1.130347	-0.631492	-1.553526
H	0.371275	-0.998228	0.874979
H	-6.672680	-1.990468	0.739689
H	-6.017190	-1.836580	-0.941022
H	-7.028701	-0.508038	-0.239915
H	4.120353	0.368825	1.418483
H	2.439380	0.053524	2.020948
H	2.165181	3.432857	2.106782
H	-1.031703	-1.384873	-1.743526

تصميم طلائع الجابابنتين بالطرق الحسابية

إعداد: هنادي عبد الكريم حسني سنقرط

إشراف: أ.د. رفيق قرمان

الملخص:

ان اكتشاف آليات عمل عدد من نماذج الإنزيمات (عملية داخل الجزيئات) ساهم في تصميم روابط كيميائية فعالة يمكن ربطها تساهمياً بالأدوية منتشرة الاستخدام والتي لها القدرة على إطلاق الدواء الفعال كيميائياً وليس بواسطة الإنزيم. يعتمد تطبيق هذه الطريقة في تصميم الطلائع على استخدام الحسابات المحوسبة و التي تقوم على أساليب الميكانيكا الجزيئية (MM2) ومدارات الجزيئات. وقد طبقت بنجاح على مجموعة واسعة من الأدوية للتغلب على بعض المشاكل الدوائية والصيدلانية ذات الصلة.

باستخدام المدار الجزيئي DFT على مستوى B3LYP 6-31G (d, p) وحسابات الميكانيكا الجزيئية لعملية نقل البروتون ضمن جزئي في عدد من نماذج الإنزيم للعالم كاربني تم تصميم عدد من طلائع الجابابنتين بهدف الحصول على دواء ذو فعالية عالية للوصول إلى الدورة الدموية في الجسم مقارنة مع الدواء الأم. كما وتم تحديد العوامل التي تلعب دورا في سرعة عملية فك الرباط وإطلاق الدواء الفعال

لقد وجد أن سرعة التحويل الداخلي لطلائع الجابابنتين تعتمد بشكل كبير على طاقة الاجهاد energy strain لكل من المتفاعلات و رباعية الاسطوح المتوسطة، ولا يوجد أي علاقة بين معدل تحلق جزيئي داخلي و المسافة بين الذرة الساحبة للكروونات و الذرة المعطية

للكترونات ومن هنا نستنتج ان سرعة التحويل الداخلي لطبيعة الجابابنتين لاطلاق الدواء الفعال
يمكن أن نتحكم به وذلك من خلال اختيار طبيعة الرابط الذي يتم ربطه بالدواء لعمل الطبيعة.